Cellular/Molecular

Prefrontal Cortex HCN1 Channels Enable Intrinsic Persistent Neural Firing and Executive Memory Function

Sébastien J. Thuault,[1] Gaël Malleret,[2] Christine M. Constantinople,[1] Russell Nicholls,[1] Irene Chen,[1] Judy Zhu,[1] Andrey Panteleyev,[1] Svetlana Vronskaya,[1] Matthew F. Nolan,[3] Randy Bruno,[1,4] Steven A. Siegelbaum,[1,4] and Eric R. Kandel[1,4,5]

[1]Department of Neuroscience, Columbia University, New York, New York 10032, [2]UMR CNRS 5167, Faculté de Médecine Laënnec, Lyon 69372, France, [3]Centre for Integrative Physiology, University of Edinburgh EH8 9XD, United Kingdom, and [4]The Kavli Institute for Brain Science and [5]Howard Hughes Medical Institute, Columbia University, New York, New York 10032

In many cortical neurons, HCN1 channels are the major contributors to I_h, the hyperpolarization-activated current, which regulates the intrinsic properties of neurons and shapes their integration of synaptic inputs, paces rhythmic activity, and regulates synaptic plasticity. Here, we examine the physiological role of I_h in deep layer pyramidal neurons in mouse prefrontal cortex (PFC), focusing on persistent activity, a form of sustained firing thought to be important for the behavioral function of the PFC during working memory tasks. We find that HCN1 contributes to the intrinsic persistent firing that is induced by a brief depolarizing current stimulus in the presence of muscarinic agonists. Deletion of HCN1 or acute pharmacological blockade of I_h decreases the fraction of neurons capable of generating persistent firing. The reduction in persistent firing is caused by the membrane hyperpolarization that results from the deletion of HCN1 or I_h blockade, rather than a specific role of the hyperpolarization-activated current in generating persistent activity. *In vivo* recordings show that deletion of HCN1 has no effect on up states, periods of enhanced synaptic network activity. Parallel behavioral studies demonstrate that HCN1 contributes to the PFC-dependent resolution of proactive interference during working memory. These results thus provide genetic evidence demonstrating the importance of HCN1 to intrinsic persistent firing and the behavioral output of the PFC. The causal role of intrinsic persistent firing in PFC-mediated behavior remains an open question.

Introduction

A fundamental goal of neuroscience is to define how electrical activity in specific neural circuits mediates complex behavior. Studies of the HCN1 channel subunit, which is a major determinant of the hyperpolarization-activated cation current, I_h, in cortical neurons, have demonstrated how a single channel expressed in distinct neural circuits can play distinct roles in neural activity and memory depending on cellular context. In cerebellar Purkinje neurons, HCN1 prevents excessive membrane hyperpolarization during inhibition, which may contribute to the function of HCN1 as a permissive gate of cerebellar motor learning (Nolan et al., 2003). In contrast, in hippocampal CA1 pyramidal neurons, HCN1 constrains dendritic integration of excitatory inputs and long-term potentiation (LTP), and also constrains hippocampal-dependent spatial learning and memory (Nolan et al., 2004). Here we investigate the importance of HCN1 in a distinct form of cellular activity and memory: persistent neural firing of prefrontal cortex (PFC) pyramidal neurons and the behavioral performance of working memory tasks.

Working memory enables us to remember and process information over short periods of time on the order of seconds (Goldman-Rakic, 1995; Baddeley, 2003; Jonides et al., 2008). Although the physiological mechanisms underlying working memory are not understood, persistent firing of cortical neurons in response to a transient stimulus is an attractive mechanism for short-term information storage (Fuster and Alexander, 1971; Niki, 1974; Niki and Watanabe, 1976; Watanabe, 1981; Sakurai and Sugimoto, 1986; Quintana et al., 1988; Funahashi et al., 1989; Miller et al., 1996; Jung et al., 1998; Baeg et al., 2003).

Two major neural mechanisms have been proposed to account for persistent firing (Wang, 2001). The first involves reverberatory activity in a network of neurons by means of recurrent synaptic connections, such as those that are important for the generation of up and down states, which correspond to periods of high and low synaptic activity, respectively (Steriade et al., 1993b; Sanchez-Vives and McCormick, 2000; Cossart et al., 2003). The second mechanism of persistent firing involves the intrinsic membrane conductances of neurons and does not require fast synaptic transmission (Schwindt et al., 1988; Egorov et al., 2002).

Received May 6, 2012; revised May 4, 2013; accepted May 29, 2013.

Author contributions: S.J.T., G.M., C.M.C., R.N., J.Z., M.F.N., R.B., S.A.S., and E.R.K. designed research; S.J.T., G.M., C.M.C., R.N., I.C., J.Z., A.P., S.V., and R.B. performed research; S.J.T., G.M., C.M.C., J.Z., and R.M.B. analyzed data; S.J.T., S.A.S., and E.R.K. wrote the paper.

This work was supported by the Howard Hughes Medical Institute, grants R01 MH045923 and MH80745 from National Institutes of Health (E.R.K. and S.A.S.), and a National Alliance for Research on Schizophrenia and Depression Young Investigator Award (S.J.T.).We are grateful to Bina Santoro, Eleanor Simpson, Christoph Kellendonk, Pierre Trifilieff, Ilias Pavlopoulos, Alexei Morozov, Pablo Jercog, Joseph Rayman, Harshad Vishwasrao, Vivien Chevaleyre, Rebecca Piskorowski, and Alexander Arguello for technical advice, reagents, and discussions about this manuscript. We also thank Deqi Yin and Brittany Dubose for expert technical assistance.

Correspondence should be addressed to either of the following: Eric Kandel, Department of Neuroscience, Columbia University, New York, NY 10032, E-mail: erk5@columbia.edu; or Steven Siegelbaum, Department of Neuroscience, Columbia University, New York, NY 10032, E-mail: sas8@columbia.edu.

DOI:10.1523/JNEUROSCI.2427-12.2013

 0270-6474/13/3313583-17$15.00/0

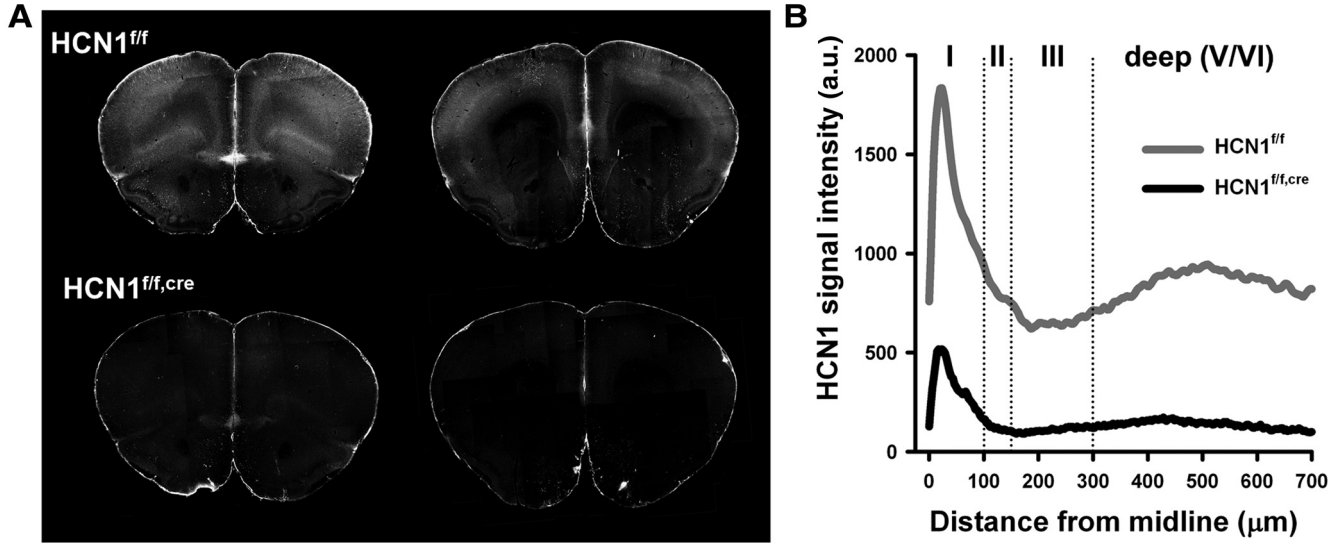

Figure 1. Laminar profile of expression of HCN1 in the PFC and its deletion in the HCN1 $^{f/f,cre}$ mouse. ***A***, HCN1 immunofluorescence in rostral (left) and caudal (right) coronal slices from the frontal brain of HCN1 $^{f/f}$ (control) and HCN1 $^{f/f,cre}$ (KO) mice. ***B***, Distribution of HCN1 immunoreactivity across the different layers of the mPFC. Note the large reduction in KO mice in HCN1 signal in layer I, the site to which layer V pyramidal neurons extend their apical dendritic tuft.

Although up states and intrinsic persistent firing have been studied extensively, there is little evidence implicating either of them in the behavioral function of the PFC (Wang et al., 2007 and 2011). As one prominent role of I_h in certain cells in the heart and in the brain is to serve as a pacemaker current to drive rhythmic firing (Robinson and Siegelbaum, 2003), I_h is an interesting candidate for generating persistent activity and regulating PFC function. We have therefore examined the importance of HCN1 in prefrontal cortical neuron up states and intrinsic persistent firing, and in PFC-dependent behavior in mice using restricted genetic deletions. Our results indicate that HCN1 is necessary for intrinsic persistent neural firing in layer V neurons in the medial PFC (mPFC) and for the executive function of the PFC during working memory episodes.

Materials and Methods

HCN1 forebrain-restricted knock-out (KO) animals (HCN1 $^{f/f,cre}$) and their control littermates (HCN1 $^{f/f}$) bred in-house were used in this study. In some experiments wild-type C57BL/6J mice from The Jackson Laboratory were used, as noted. The generation of the KO line was described previously (Nolan et al., 2004). The HCN1 mice had a mixed average 50/50% 129SvEv/C57BL/6J background. They were bred and maintained under standard conditions, consistent with National Institutes of Health guidelines and Institutional Animal Care and Use Committee approved protocols. Throughout the paper, means are stated as mean ± SEM. All mice used in this study were males.

Immunohistology processing and imaging

Under terminal anesthesia, the mice were transcardially perfused with PBS followed by 4% paraformaldehyde (PFA). The brains were then dissected out and postfixed overnight at 4°C in PFA. Fifty micrometer sections were cut on a vibrating slicer and processed using standard immunocytochemical techniques (Nolan et al., 2007). The following primary antibodies were used: rat monoclonal HCN1 antibody (a generous gift from F. Müller and B. Kaupp, Institute for Neuroscience and Biophysics, Jülich, Germany; dilution 1/50) and rabbit polyclonal Cre antibody (produced in the laboratory by Christoph Kellendonk; 1/1500). Secondary antibodies used include goat polyclonal anti-rat or anti-rabbit coupled to Rhodamine-Red-X or Cy5 (purchased from Jackson ImmunoResearch; 1/400). All images were taken using a laser-scanning confocal microscope.

In vitro *electrophysiology*

Coronal frontal brain slices were obtained from 1.5- to 3.5-month-old mice using standard brain slicing methods. Briefly, the animals were killed by cervical dislocation, followed by decapitation and dissection of the brain out of the cranium. The brain was quickly placed in cold-modified artificial CSF (ACSF) containing the following (in mM): 10 NaCl, 195 sucrose, 2.5 KCl, 0.5 $CaCl_2$, 7 $MgCl_2$, 1.25 Na_2PO_4, 25 $NaHCO_3$, 10 glucose, and 2 Na-pyruvate, osmolality 325 mOsm for 3–4 min. Slices (300–400 μm thick) were obtained using a Vibratome 3000 and placed in a beaker of warm (32°C) standard ACSF containing the following (in mM): 125 NaCl, 2.5 KCl, 2 $CaCl_2$, 1 $MgCl_2$, 1.25 Na_2PO_4, 25 $NaHCO_3$, 25 glucose, and 2 Na-pyruvate, osmolarity 305 mOsm for ~30 min. Slices were then cooled to room temperature for another 30 min before recordings were initiated. All intracellular recordings were obtained using the whole-cell patch-clamp technique in a submerged chamber continuously perfused with warm ACSF at 34°C. The soma of layer V pyramidal neurons were identified and patch-clamped after visual approach of the recording pipette using a combination of infrared light and differential interference contrast (DIC) optics. Patch electrodes had a resistance of 2–5 MΩ when filled with the following intracellular solution (in mM): 130 $KMeSO_4$, 10 KCl, 10 HEPES, 4 NaCl, 0.1 EGTA, 4 MgATP, 0.3 Na_3GTP, and 10 Na_2-phosphocreatine, osmolarity 305, pH adjusted to 7.25 with KOH. Recordings were terminated if the series resistances exceeded 20 MΩ for voltage-clamp recordings and 40 MΩ for current-clamp recordings. Concentric bipolar tungsten electrodes were used for synaptic stimulation. The signals were digitized at 10–50 kHz and low-pass filtered at 1–4 kHz.

Induction of intrinsic persistent activity was initiated by bath application of the following drugs (in μM): 10 carbachol (CCh), 10 NBQX, 50 AP5, and 50 picrotoxin. When the membrane potential was stable, a series of current injection steps (200 pA for 500 ms, 400 pA for 500 ms, 400 pA for 1 s, 400 pA for 2 s, 400 pA for 4 s, 600 pA for 2 s, 600 pA for 4 s, 600 pA for 6 s, and 800 pA for 6 s; sometimes intermediate values were used) were applied to the soma with interstimulus intervals of ~1 min. The slow afterdepolarization (sADP) following the depolarization was sometimes accompanied by transient spiking, which prohibited the accurate measurement of its amplitude. These experiments were excluded from the analysis of the sADP ($n = 2$ in wild-type and $n = 8$ in KO mice; see Fig. 6*A*,*B*).

Recordings were analyzed using IGOR Pro (WaveMetrics) or Clampfit (Molecular Devices). I_h currents were fitted with one or two exponentials $[(A_1 \times {}_{\exp(-1/\tau fast)}) + A_2 \times \exp(1/\tau_{slow})]$. Student's *t* tests, Gehan—

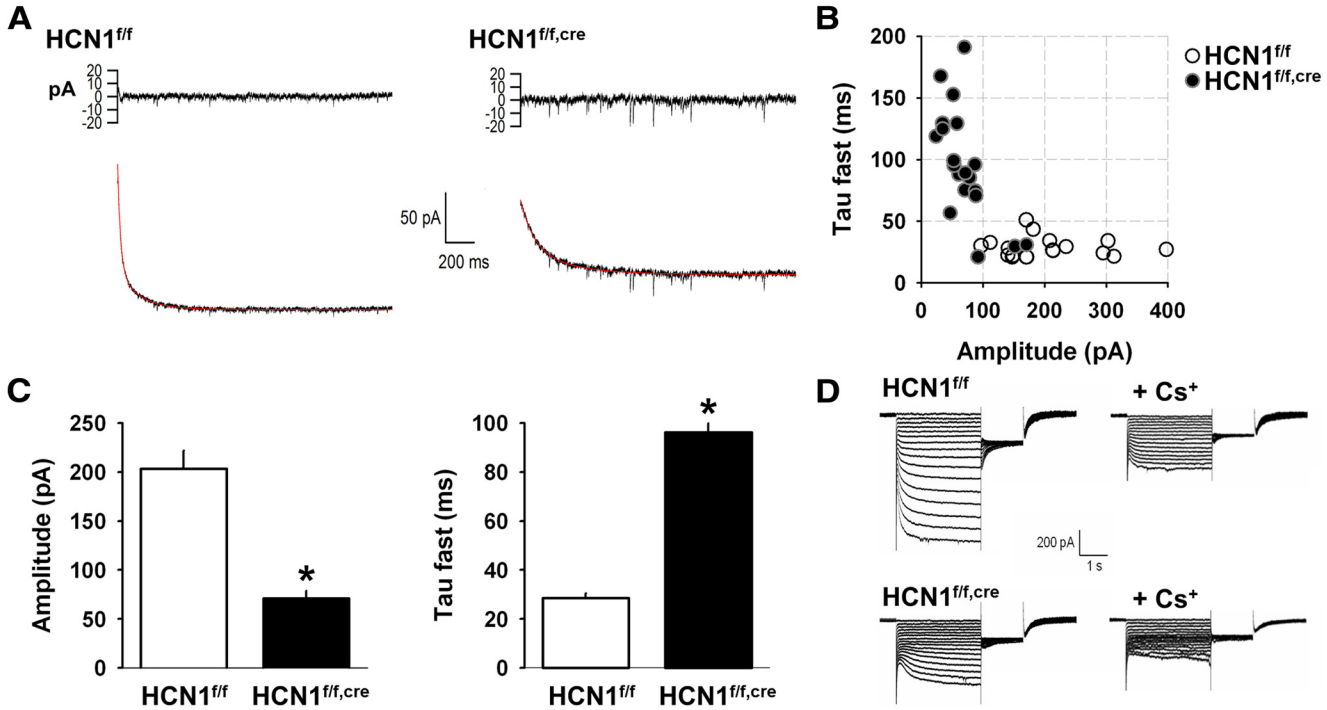

Figure 2. Deletion of HCN1 decreases the magnitude and slows the activation of I_h in mPFC layer V pyramidal neurons. ***A***, Example traces of I_h recorded at 34°C in neurons from HCN1$^{f/f}$ and HCN1$^{f/f,cre}$ mice (bottom). I_h was activated by a 60 mV hyperpolarizing step from a holding potential of −52 mV. Current traces were fitted by a curve with two exponential components (superimposed in red on the traces). The residuals of the fit are shown above the current traces. ***B***, Properties of I_h recorded in neurons from control (○; $n = 18$) and KO (●; $n = 20$) mice. For each neuron the fast time constant of activation was plotted against the maximal current amplitude of I_h following a step to −112 mV. Note that the data fall into two clusters that segregate with genotype, with the exception of data from three neurons from the KO mice, whose I_h properties were similar to those of the control group (see text for discussion). ***C***, Comparison of the average values of I_h amplitude ($p < 0.00001$, unpaired *t* test) and fast time constant of activation (τ fast, $p < 0.00001$, unpaired *t* test) in neurons from control and KO mice ($n = 18$ and 20, respectively). ***D***, Representative example from a distinct set of experiments at room temperature showing the blockade of I_h by Cs^+ (4 mM) in layer V mPFC pyramidal neurons from control (top) and HCN1 KO mice (bottom). I_h was activated by a series of hyperpolarizing voltage-clamp steps from −50 to 115 mV in 5 mV increments. Right, Currents in the presence of 4 mM external Cs^+. I_h was pharmacologically isolated by using blockers of inward rectifier K^+ channels (1 mM Ba^{2+}), voltage-gated K^+ channels (1 mM 4-aminopyridine and 5 mM tetraethylammonium), and voltage-gated Na^+ channels (1 μM tetrodotoxin).

Breslow–Wilcoxon and two-way repeated-measures ANOVA followed by Bonferroni *post hoc* tests were used to determine statistical significance.

In vivo *electrophysiology*

Patch pipettes (4–7 MΩ) were pulled from borosilicate glass and tip-filled with the following (in mM): 135 K-gluconate, 10 HEPES, 10 Na_2 phosphocreatine, 4 KCl, 4 MgATP, 0.3 guanosine triphosphate, and 0.2–0.4% biocytin (pH 7.2, osmolarity 291). Pipette capacitance was neutralized before break-in, and access resistance was 25–45 MΩ. Recordings were digitized at 32 kHz. Analyses were performed using custom routines in MATLAB. To classify membrane fluctuations as belonging to up or down states, we used an algorithm that compares two moving averages having different window sizes (Seamari et al., 2007).

Behavior

Delayed non-matched to place. The animals used in the working memory experiments were singly housed and food deprived to 85% of their *ad libitum* weight by daily adjustment of their food intake. The experimenter was blind to the genotypes or viral injections. The age of the animals ranged from 4 to 6 months for the forebrain-restricted KO study and 8 to 10 months for the PFC-restricted KO study.

The delayed non-match to place (DNMP) task was performed in an 8-arm radial maze that was similar to a previous study (Saxe et al., 2007). Pretraining consisted of a random-foraging task with all eight arms opened and baited, during which the mice could make up to 10 arm visits to retrieve the food pellets (5 d, 1 trial per day, maximum trial duration of 360 s). During the DNMP procedure, each trial consisted of a sample phase and a choice phase separated by an intra-trial delay. In the sample phase, mice were allowed to explore and retrieve the food from one of the eight arms; then a delay ensued in which the mice were isolated from the maze in a delay box. After the delay, the choice phase started by placing the mice back in the maze in an arm that was either facing the goal or the non-goal arm (randomly determined). An intertrial interval of 2 min separated two consecutive trials. This testing was performed in two versions of the same task. In the standard version consecutive trials used different pairs of adjacent arms (DP). In the modified version the same pair of adjacent arms was used for all trials (SP), with the initial baited arm chosen randomly for each trial. Each version of the task began with a training phase using a 10 s delay and consisted of 6 trials per day for 8 to 12 d (4 to 6 blocks). After this initial phase, longer intra-trial delays were introduced every 2 d (with progressive delays of 20, 30, and 50 s). Statistical analysis was performed using two-way repeated-measures ANOVA with the genotype as the source of variation followed by *post hoc* Bonferroni tests for the training phase. Student's *t* tests were used for the delay results. One-way ANOVA was used for within-group comparison of trial performance. The initial training period for the virally injected animals was prolonged by two blocks when four blocks of training were not sufficient to reach a level of performance similar to that of the forebrain-restricted animals in the standard version.

Five-choice serial reaction time task. Animals were trained in four operant 5-choice boxes outfitted for mice (Med Associates). The animal's weight was maintained at ~85% of *ad libitum* body weight throughout training and testing with rodent chow. Condensed milk was used as reinforcement. Mice performed two daily training sessions 5 d a week. Each session lasted 30 min or consisted of 50 trials, whichever occurred first. Each session was initiated by retrieving a single dip from the food receptacle. Each trial began with the random illumination of one of the five nose-poke holes. Trials were separated by an inter-trial interval (ITI) of 5 s. A correct response was made if the mouse poked its nose into a hole while the hole was illuminated, or within 5 s of

illumination offset. When a correct response was made, the dipper cup was raised, allowing the mouse access to the liquid food reinforcer. Nose pokes into an incorrect dark hole were recorded as errors and resulted in a 10 s timeout that was signaled by the house light being turned off and no access to the liquid dipper. Timeouts were also imposed when the mouse failed to nose poke into any hole (omissions) and when the mouse nose poked during the ITI (premature/impulsive responses). Multiple nose pokes into a correct hole (perseverative responses) were recorded but had no scheduled consequences. Mice were trained on a stepwise progression in which stimulus duration was incrementally decreased as the mice reached the performance criteria of 20% omissions and 80% accuracy for five consecutive sessions. The sequence of stimulus durations during training was 15, 8, 4, 2, and 1 s. After training, demands on attention were tested by shortening stimulus duration to 0.5, 0.25, and 0.125 s. Statistical significance was assessed using unpaired Student's *t* test.

Virus design and production

GFP (LV-GFP)- or Cre (LV-Cre)-expressing lentivirus was produced using the following methods. The NLS-Cre coding sequence was amplified using PCR primers Cre-Xma-for and Cre-RI-rev from the template pHD2-Cre1 (a gift from Christoph Kellendonk, Columbia University, New York, NY). The product was digested with XmaI and EcoRI and substituted for the GFP-containing AgeI/ EcoRI fragment of the lentiviral vector pFCK(0.4)GW (a gift from Pavel Osten, Cold Spring Harbor Laboratory, Cold Spring Harbor, NY; Dittgen et al., 2004). Lentiviruses were produced by cotransfection of 20 μg of vector plus 10 μg each of helper plasmids pMD2.G, pMDLg/RRE, and pRSV-rev (Addgene; Dull et al., 1998) in 293FT cells using Lipofectamine 2000 (Invitrogen). Forty-eight hours after transfection, virus-containing supernatants were passed through a filter with 0.45 mm pore size and concentrated by ultracentrifugation at 88,000 $\times$ *g* for 3 h at 4°C over a 20% sucrose cushion. Pelleted viral particles were resuspended in D-PBS containing Mg^{2+} and Ca^{2+} (Invitrogen) to yield solutions with 1×10^8 and 1×10^9 infectious units per milliliters.

The following primer sequences were used: CRE-Xma-for: CTAAGCTTCCCGGGCTCGACCATGCCCAAG; Cre-RI-rev: ATTGAATTCTTAATCGCCATCTTCCAGCAGGC.

The AAV-flex-GFP viruses used for *in vitro* electrophysiology were purchased from Penn Vector (catalog #V1675). Their serotype was 2/1, the GFP open-reading-frame was inverted, flanked by loxP sequences, and driven by the CAG promoter.

Surgical and viral injection procedures

Viral injections were performed in a biohazard level 2 biochemical cabinet. Animals were anesthetized with a mixture of ketamine and xylazine via intraperitoneal injection and operated on using standard sterile conditions. A small rectangular window was drilled in the skull to allow the penetration of a fine glass pipette (8–15 μm inner diameter) containing the solution of viral particles. Viral injection was performed by applying pressure to a syringe to eject 0.5–1 μl of solution delivered bilaterally at the following three coordinates relative to bregma: anteroposterior 1.85, 2.15, 2.45; ventrodorsal 1.6, 1.5, 1.4; mediolateral 0.4 for all three sites. The rate of injection ranged on average from 0.1 to 0.2 μl/min. Following the injections, the skull was covered with triple antibiotic ointment, the wound sutured, and the animal injected with the analgesic buprenorphine (0.05–0.1 mg/kg, s.c.), once during initial recovery and then 12–24 h later.

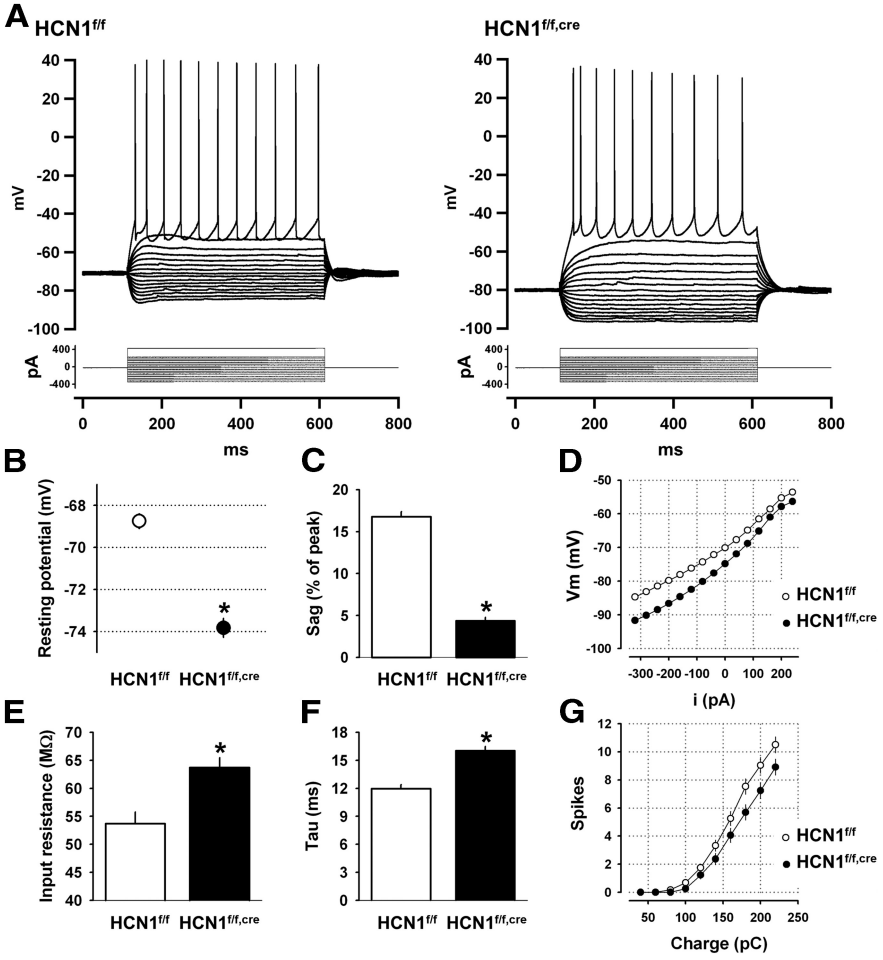

Figure 3. HCN1 contributes to the intrinsic electrophysiological properties of mPFC layer V pyramidal neurons. ***A***, Membrane potential responses of two representative neurons from control and KO mice in response to a series of hyperpolarizing and depolarizing current steps. ***B–G***, Comparison of various intrinsic membrane parameters of mPFC layer V pyramidal neurons from control ($n = 28$) and HCN1 KO mice ($n = 35$). HCN1 deletion causes: (***B***) Hyperpolarizing shift in resting potential ($p < 0.00001$, unpaired *t* test); (***C***) Reduced voltage sag in response to hyperpolarizing current step (measured as the percentage of the peak voltage deflection in response to a 1 s −400 pA step, $p < 0.00001$, unpaired *t* test); (***D***) Hyperpolarizing shift in the subthreshold current input versus voltage output relationship (I/O curve); (***E***) Increased input resistance (measured near rest, $p < 0.001$, unpaired *t* test); (***F***) Increased membrane time constant ($p < 0.00001$, unpaired *t* test); and (***G***) No significant change in excitability, measured as number of spikes fired in response to increasing depolarizing current steps.

Results

Expression profile of HCN1 in the PFC

As a first step in assessing the role of I_h in PFC, we examined mice in which HCN1 was deleted selectively in the forebrain ($HCN1^{f/f,cre}$), as previously described (Nolan et al., 2003, 2004). The expression of Cre was driven by the CaMKIIα promoter, thereby limiting HCN1 deletion to forebrain neurons at relatively late postnatal developmental stages (>P14). We first compared HCN1 protein expression in control ($HCN1^{f/f}$) and forebrain-restricted KO ($HCN1^{f/f,cre}$) littermates using immunohistochemistry. Our results show that HCN1 protein is highly expressed in both deep and superficial layers of PFC in control animals (Fig. 1*A*,*B*). This is consistent with previous results showing that the highest levels of mRNA expression are in neocortical layer V neuron soma (Santoro et al., 2000) and that HCN1 protein is strongly targeted to layer V neuron distal den-

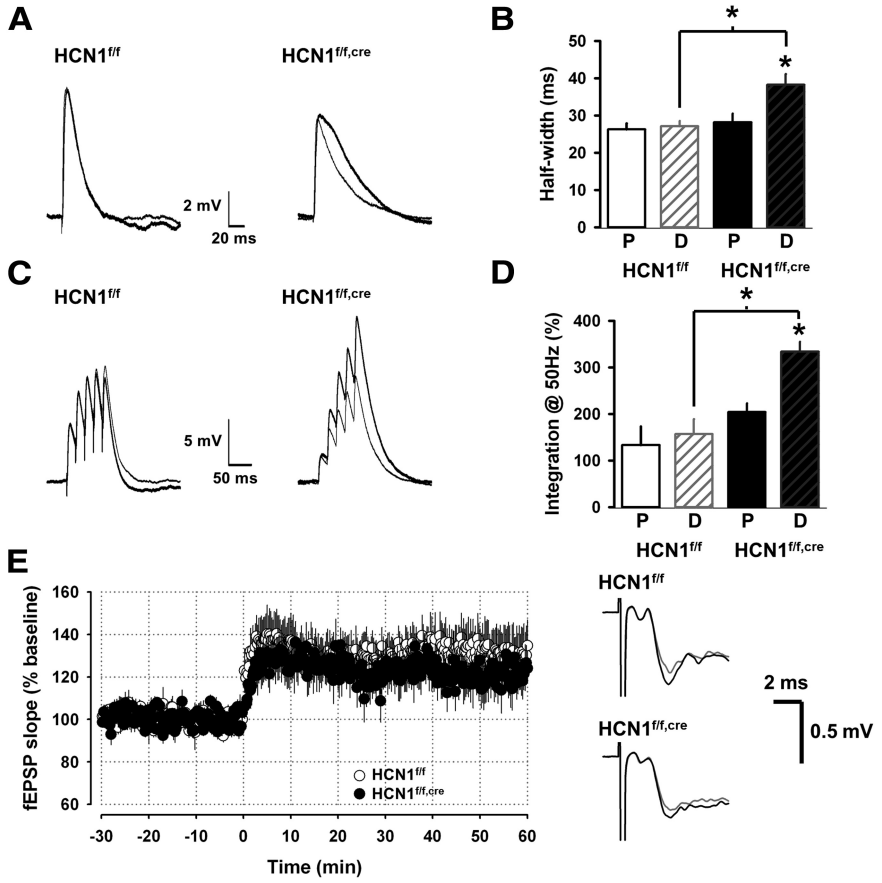

Figure 4. HCN1 influences the time course and temporal summation of synaptic potentials evoked by distal stimulation but not their LTP. ***A***, Average PSPs (average of 8–10 responses) recorded in the soma of two cells from control and KO mice in response to extracellular stimulation in layer I (distal, thick trace) or layer V (proximal, thin trace). ***B***, Comparison of the half-width of the somatic PSPs in neurons from control mice ($n = 4$ for proximal stimulation, P; $n = 8$ for distal stimulation, D) and KO mice ($n = 4$ for P and 7 for D). PSP half-widths in response to distal stimulation were significantly larger in KO versus control mice ($p < 0.01$, unpaired *t* test). Half-widths of PSPs elicited by distal versus proximal stimulation were significantly different when compared in KO mice ($p < 0.05$, paired *t* test) but not control mice ($p = 0.72$, paired *t* test). ***C***, Temporal summation of somatic PSPs elicited by proximal and distal stimulation in the presence and absence of HCN1. Example traces show PSPs elicited by a burst of five stimuli at 50 Hz. ***D***, Comparison of the normalized summation of PSPs elicited by proximal and distal stimulation in neurons from control and KO mice. Summation defined as $S = (EPSP5 - EPSP1)/EPSP1) \times 100\%$), where EPSP5 is the peak amplitude of the fifth EPSP of the burst and EPSP1 is the amplitude of the first EPSP. Summation of EPSPs elicited by distal stimulation in KO mice was significantly greater compared with control mice ($p < 0.01$, unpaired *t* test; Control, $n = 8$; KO, $n = 5$). Summation of EPSPs elicited by proximal stimulation was not significantly different between control and KO mice ($p = 0.66$, unpaired *t* test; Control, $n = 4$; KO, $n = 4$). ***E***, Average slope of the distal field EPSPs (fEPSPs; recorded in layer I) before and after induction of LTP using theta-burst stimulation in layer I (3 trains of 10 bursts at 5 Hz, each burst consisted of 8 stimuli at 100 Hz). HCN1 KO had no effect on the magnitude of LTP. These recordings were performed in the presence of 50 μM picrotoxin, a $GABA_A$ receptor blocker. Right, Example traces of the distal fEPSP recorded in layer I in PFC slices from control and KO mice before (gray) and 60 min after induction of LTP (black).

drites, which are present in layer I (Santoro et al., 2000; Lörincz et al., 2002). Upon HCN1 deletion, channel expression is greatly reduced but not eliminated, because of the mosaic nature of expression of Cre recombinase.

Contribution of HCN1 to prefrontal I_h

We next examined the contribution of HCN1 to I_h in regular spiking layer V pyramidal neurons in mPFC by comparing whole-cell voltage-clamp current recordings from neurons in control ($HCN1^{f/f}$) and forebrain-restricted HCN1 KO ($HCN1^{f/f,cre}$) mice. Pyramidal cells in layer V of the PFC form a heterogeneous population of cells (Dembrow et al., 2010). We restricted our analysis to regular-spiking neurons as preliminary recordings showed that they consistently displayed a prominent sag mediated by a fast I_h under voltage clamp (Day et al., 2005), which is characteristic of the expression of HCN1 in pyramidal neurons (Santoro et al., 2000). These cells had a large soma and displayed a recognizable firing pattern in response to a modest depolarization, consistently exhibiting regular/non-adapting firing, often following an initial spike doublet, which made them easy to distinguish from other pyramidal cell types in this layer that showed pronounced spike frequency adaptation. In control slices kept at 34°C, hyperpolarizing voltage steps elicited a large I_h (203 ± 19 pA for a step from -52 mV to -112 mV, $n = 18$), whose amplitude increased with increasing levels of hyperpolarization. A fit to the time course of activation of I_h required the sum of a fast ($\tau_{fast} = 28.5 \pm 1.9$ ms) and slow ($\tau_{slow} = 385 \pm 39$ ms) exponential component (Fig. 2*A*, left), likely reflecting the presence of fast HCN1 and slower HCN2 channels, as previously described in CA1 pyramidal neurons (Santoro et al., 2000; Nolan et al., 2004). In contrast, recordings of I_h from the $HCN1^{f/f,cre}$ KO mice revealed two distinct populations of neurons (Fig. 2*B*). In the majority of neurons (17 of 20), the amplitude of I_h was small (<100 pA) and its time course of activation was slow ($\tau_{fast} > 50$ ms; Fig. 2*A*, right). A minority of neurons (3 of 20) in the KO mice displayed a larger I_h with fast kinetics that were similar to those observed in control mice. This likely reflects the mosaic nature of Cre expression, which is expressed in ~90% of forebrain pyramidal neurons in the $HCN1^{f/f,cre}$ mice (Nolan et al., 2004). On average, the mPFC layer V neurons from $HCN1^{f/f,cre}$ mice exhibited a 60% decrease in the amplitude of I_h ($i = 71 \pm 8$ pA, $n = 20$) and a threefold slowing in its kinetics of activation ($\tau_{fast} = 96 \pm 10$ ms and $\tau_{slow} = 268 \pm 39$ ms; Fig. 2*C*). We obtained similar results in a distinct set of experiments conducted at room temperature, in conditions in which I_h was pharmacologically isolated by application of blockers of Na^+, K^+, and Ca^{2+} channels as well as blockers of fast synaptic transmission (Fig. 2, see legend). Such experiments confirmed that the inward current was indeed caused by I_h, as it was inhibited by the I_h blocker cesium (Fig. 2*D*). These results indicate that HCN1 is the predominant subunit supporting the generation of I_h in PFC pyramidal neurons. The presence of a residual slow current in the $HCN1^{f/f,cre}$ neurons likely is due to the presence of HCN2 subunits (Day et al., 2005).

HCN1 influences the intrinsic membrane properties of prefrontal cortical neuron

I_h is known to contribute to several intrinsic membrane properties such as the resting potential, input resistance, and membrane time constant (Robinson and Siegelbaum, 2003). To examine how HCN1 contributes to these properties in layer V mPFC neurons, we next performed somatic whole-cell current-clamp recordings from control and KO mice. Loss of HCN1 induced a hyperpolarizing shift in the resting membrane potential and an

increase in input resistance and membrane time constant, consistent with the observed reduction in I_h (Fig. 3). In addition, in neurons from HCN1 KO mice, the size of the depolarizing sag in response to a hyperpolarizing current step, characteristic of the activation of I_h, was greatly reduced (Fig. 3*A*,*C*). In contrast, deletion of HCN1 did not significantly alter neuronal excitability, although neurons from mutant mice showed a slight but not significant decrease in the number of spikes elicited by depolarizing current steps compared with control littermates (Fig. 3*G*).

The role of HCN1 in the temporal integration of distal synaptic inputs

In both neocortical and CA1 pyramidal neurons, HCN channels can affect temporal integration of synaptic inputs (Magee, 1998, 1999; Williams and Stuart, 2000; Day et al., 2005; Atkinson and Williams, 2009) and the expression of long-term synaptic plasticity (Nolan et al., 2004). To determine whether HCN1 contributes to similar properties in prefrontal neurons, we measured the time course and temporal summation of layer V neuron somatic postsynaptic potentials (PSPs) recorded under whole-cell current clamp in response to stimulation of proximal (layer V) or distal synaptic inputs (layer I). Previous studies have shown that HCN1 has a significantly greater effect on distal versus proximal PSPs because HCN1 channels are most strongly expressed in the distal dendrites.

We found that the half-width of PSPs elicited by distal stimulation was significantly longer in neurons from the HCN1 KO mice ($HCN1^{f/f,cre}$) compared with neurons from control mice ($HCN1^{f/f}$), consistent with the effect of I_h to decrease the membrane time constant (Fig. 3*F*). In addition, whereas half-width of PSPs elicited by distal and proximal stimulation were similar in neurons from control mice, the half-width of the distal PSP was significantly longer than the half-width of the proximal PSP in neurons from the HCN1 KO mice (Fig. 4*A*,*B*). This result is consistent with previous findings that the high density of I_h and HCN1 in the distal dendrites helps normalize the time course of somatic PSPs elicited by distal versus proximal synaptic inputs (Stuart and Spruston, 1998; Magee, 1999; Nolan et al., 2004). In the absence of HCN1 the distal PSPs are prolonged relative to proximal PSPs by the passive cable properties of the dendrites. Furthermore, we found that the temporal summation of synaptic inputs to the distal dendrites in layer I was enhanced in the KO, compared with either the proximal inputs in the KO or the distal inputs in control mice (Fig. 4*C*,*D*), again consistent with previous results supporting the role of HCN1 in the temporal integration of synaptic inputs.

Previous studies in CA1 pyramidal neurons have shown that HCN1 inhibits induction of LTP at distal cortical inputs (Nolan et al., 2004). To examine whether HCN1 plays a similar role in mPFC, we recorded the layer I field EPSPs before and after induction of LTP using theta-burst stimulation of the corresponding inputs. In contrast to the results in hippocampus, the magnitude of LTP was not different between the two groups of animals (Fig. 4*E*), indicating a differential role for HCN1 in CA1 compared with layer V pyramidal cells.

Does HCN1 facilitate the generation of persistently active states?

PFC function is associated with periods of sustained firing, in particular during working memory tasks (Goldman-Rakic, 1995). Given the importance of HCN channels in certain forms of spontaneous and rhythmic firing (Mao et al., 2001; Robinson and Siegelbaum, 2003), and the important physiological changes that we observed in pyramidal neurons of the PFC in the absence of HCN1, we examined whether HCN1 deletion had an impact on the ability of mPFC layer V neurons to generate either network-dependent or intrinsic forms of persistent firing.

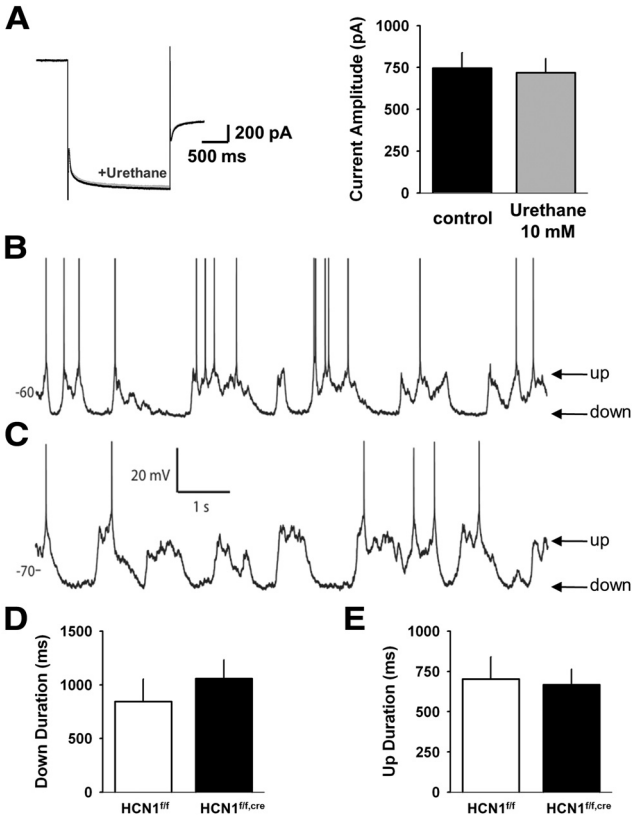

Figure 5. HCN1 deletion does not affect cortical up and down states recorded from layer V mPFC neurons. ***A***, Urethane does not block I_h in layer V mPFC neurons. I_h was recorded at physiological temperature in response to 2 s hyperpolarizing voltage steps from −50 mV to −100 mV. Currents elicited before (black trace) and in the presence of 10 mM urethane (gray trace) are superimposable (left). Average values of I_h in absence or presence of 10 mM urethane ($n = 4$) are shown on the right. ***B***, *In vivo* intracellular recording from a neuron in an anesthetized control mouse reveals prominent up and down states. ***C***, Intracellular recording of a neuron from an anesthetized KO mouse exhibits up and down state fluctuations similar to control. ***D***, Mean down state length of neurons recorded from control ($n = 9$) and KO ($n = 11$) animals. There was no significant difference between groups ($p = 0.36$, unpaired *t* test). ***E***, Mean up state length of neurons in the two groups. There was no significant difference between groups ($p = 0.82$, unpaired *t* test).

Lack of Influence of HCN1 on the dynamics of up and down state *in vivo*

Reverberatory activity in a network of neurons can occur by means of recurrent synaptic connections. Such network architecture is thought to underlie up states, periods of elevated synaptic activity, and membrane depolarization that lead to increased firing (Steriade et al., 1993b; Sanchez-Vives and McCormick, 2000; Cossart et al., 2003; Seamans et al., 2003; Compte, 2006; Haider and McCormick, 2009; Crunelli and Hughes, 2010).

To characterize the potential impact of the deletion of HCN1 on recurrent network activity, we recorded up and down states in the PFC. As up states are difficult to observe in isolated slices from adult mouse brain, we turned to the *in vivo* anesthetized mouse where robust up and down state transitions can be readily observed in cortical neurons, including those in PFC (Lavin and Grace, 2001; Dégenètais et al., 2002; Valenti and Grace, 2009).

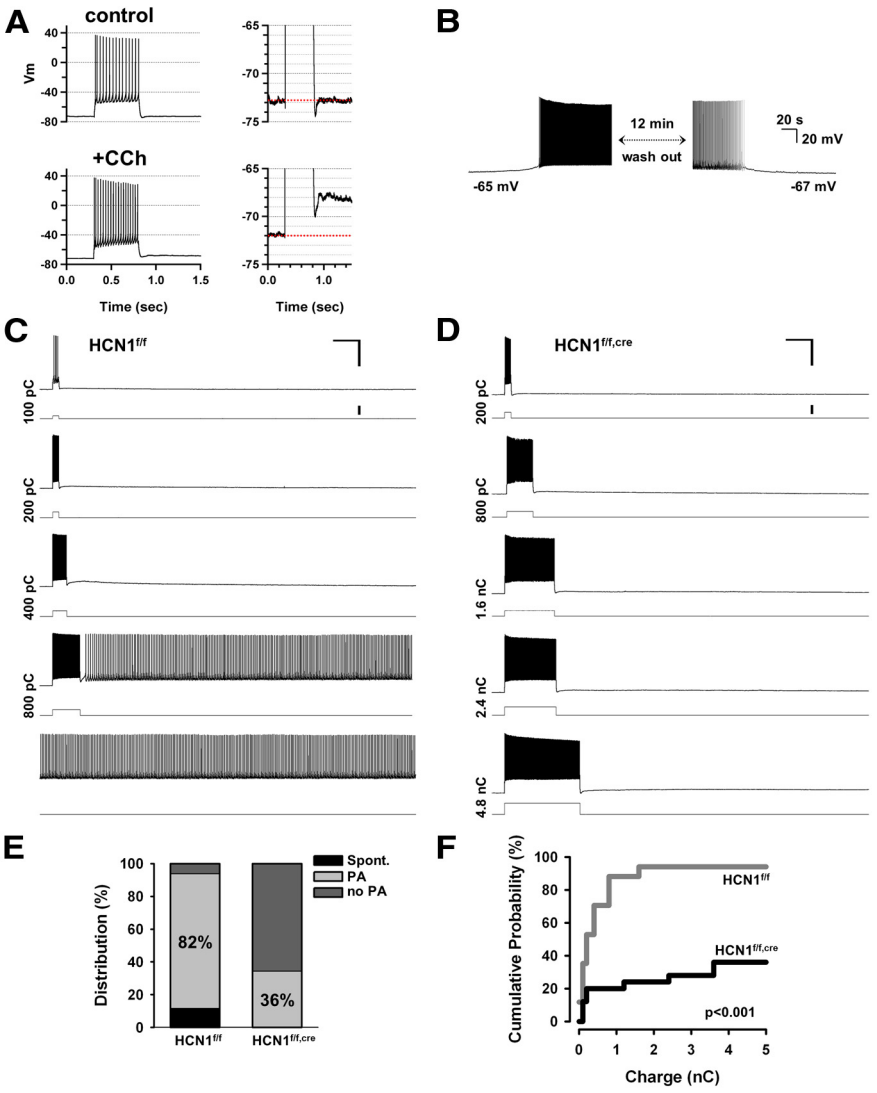

Figure 6. Deletion of HCN1 impairs the ability of mPFC layer V neurons to generate intrinsic persistent firing. ***A***, Application of muscarinic receptor agonist CCh increases action potential firing during a 500 ms depolarizing current step (left). Right, The same traces are shown on an expanded voltage scale to better illustrate the sADP following the burst of action potentials in the presence of CCh. ***B***, Example of a neuron in which CCh produced sufficient depolarization to result in spontaneous action potential firing, which stopped upon washout of CCh. The resting potential also returned to its initial level. ***C***, Representative experiment showing the induction of persistent activity in a neuron from a control mouse. Pairs of traces show membrane voltage response (top trace) to depolarizing current pulse (bottom trace). Total charge injected indicated on the left of traces. In this neuron +800 pC triggered persistent firing (shown in the fourth pair of traces). Calibration: 50 mV, 2 s, 500 pA. ***D***, Representative experiment showing lack of persistent firing in a neuron from a KO mouse. Maximum charge injected was 4800 pC. Calibration: 50 mV, 2 s, 500 pA. ***E***, Percentage of neurons generating persistent firing in control and KO mice. Black area indicates percentage of neurons that fired spontaneously in the absence of current injection. Light gray area shows percentage of neurons that could be induced to fire persistently in response to a brief depolarizing current pulse. Dark gray area represents neurons that failed to fire persistently in response to even very strong depolarizing current pulses (no PA group). Percentage of neurons exhibiting persistent activity was 82% in control ($n = 17$) and 36% for HCN1 KO mice ($n = 25$). Twelve percent of neurons from control mice and 0% of neurons from KO mice fired spontaneously. ***F***, Cumulative probability of persistent activity induction as a function of the stimulus charge. The probability curve was shifted significantly to the right and down in neurons from KO mice ($p < 0.0001$, $n = 17$ and 25 for control and KO, respectively, Gehan–Breslow–Wilcoxon test). All recordings in these and all other intrinsic persistent activity experiments were performed in the presence of the following blockers of fast synaptic transmission: NBQX (10 μM), AP5 (50 μM), and picrotoxin (50 μM), in addition to the muscarinic receptor agonist CCh (10 μM).

As I_h was shown previously to be sensitive to several anesthetic agents (Chen et al., 2005, 2009), we first tested the effect of several anesthetic agents on I_h in cortical slices. We found that urethane, widely known to produce prominent up and down states, showed negligible effects on I_h, even at concentrations higher than those required for anesthesia (Fig. 5*A*). We thus analyzed the temporal aspects of up and down state transitions using *in vivo* whole-cell recordings from deep layer pyramidal neurons in the mPFC of wild-type and forebrain-restricted HCN1 KO mice anesthetized with urethane.

Neurons from wild-type (Fig. 5*B*) and HCN1 forebrain-restricted KO (Fig. 5*C*) mice exhibited typical up and down state fluctuations in their subthreshold membrane potential. There was no significant difference between the groups in the mean duration of either the up or the down states (Fig. 5*D*,*E*; p values > 0.1). Thus, HCN1 does not substantially contribute to the dynamics of up and down states in mouse mPFC *in vivo*.

HCN1 is necessary for the intrinsic persistent firing of mPFC neurons

Intrinsic persistent firing is another form of persistent activity that relies on the recruitment of various membrane conductances that self-sustain spiking within a single cell (Schwindt et al., 1988; Andrade, 1991; Kiehn, 1991; Marder and Calabrese, 1996; Egorov et al., 2002; Derjean et al., 2005; Pressler and Strowbridge, 2006; Yoshida and Hasselmo, 2009). It requires activation of a phospholipase C-dependent signaling cascade, either through stimulation of muscarinic acetylcholine (ACh) receptors or metabotropic glutamate receptors, and the recruitment of the calcium-activated nonselective cation current (I_{CAN}), which is thought to generate a slow after-depolarization (sADP) following a burst of action potentials (Haj-Dahmane and Andrade, 1996, 1998; Egorov et al., 2002; Fransén et al., 2006; Sidiropoulou et al., 2009).

We induced intrinsic persistent activity by applying brief somatic depolarizing current injections in the presence of CCh to activate muscarinic ACh receptors, as previously described (Schwindt et al., 1988; Egorov et al., 2002). Fast synaptic transmission was blocked using APV and CNQX to inhibit NMDA and AMPA receptors and picrotoxin to block $GABA_A$ receptors.

Application of CCh (10 μM) to the slice induced an increase in excitability and the appearance of an sADP following a burst of action potentials (Fig. 6*A*). In a small number of neurons (2 of 17 neurons in control slices and none of 25 neurons in KO slices), CCh led to a large depolarization accompanied by spontaneous firing that was reversible upon washout of the agonist (Fig. 6*B*). In neurons that did not fire spontaneously, we attempted to induce persistent firing by triggering a short burst of action potentials with a depolarizing current step. The majority of these neurons exhibited an sADP whose amplitude increased as a function of stimulus strength, eventually giving rise to sustained firing outlasting the initial de-

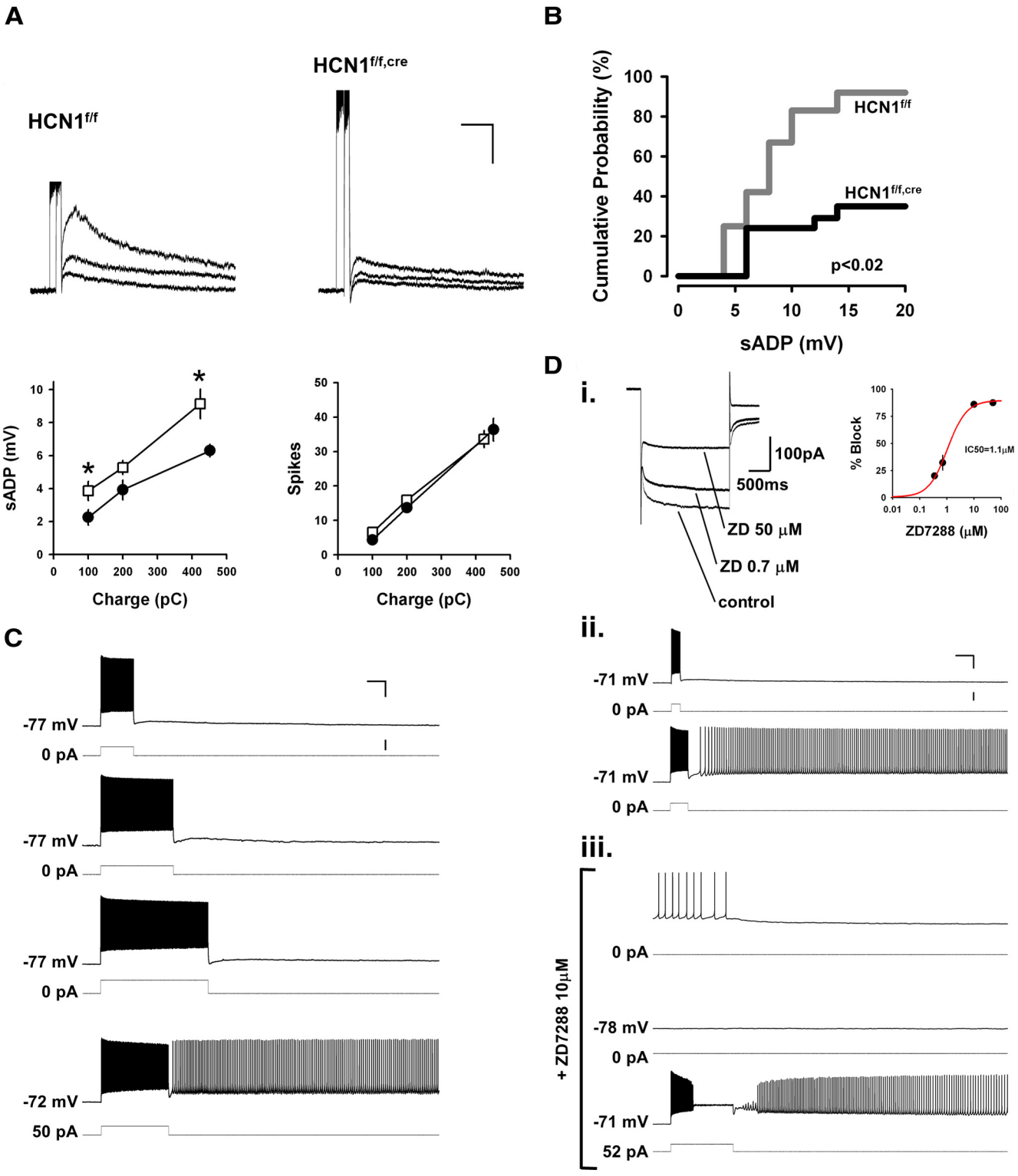

Figure 7. HCN1 promotes persistent firing in mPFC layer V neurons through tonic membrane depolarization. ***A***, Effect of deletion of HCN1 on the amplitude of the sADP. Top, Examples of voltage responses to 100, 200, and ~400 pC depolarizing current stimuli in neurons from control (left) and KO (right) mice. The ends of the stimulation epochs are aligned to superimpose the sADPs. Bottom, Left, average sADP amplitude in neurons from control (□) and KO (●) mice plotted as a function of stimulus charge. Right, Average spike count as function of charge. sADP responses to 100 and 400 pC pulses were significantly reduced by HCN1 deletion ($p < 0.04$ and $p < 0.01$, respectively, unpaired *t* tests; $n = 8–15$ in control and 20–25 in KO mice). Spike counts were identical in the two populations. Calibration: 5 mV, 3 s. ***B***, Cumulative probability of inducing persistent activity as a function of the maximum sADP amplitude observed. Maximum sADP was determined following the current step just below that needed to generate persistent firing. For neurons that did not fire persistently, maximum sADP was measured across the entire range of current pulses. Deletion of HCN1 caused a significant decrease in persistent firing, even for similar sized ADPs ($p < 0.02$, $n = 12$ and 17 for control and KO, respectively, Gehan–Breslow–Wilcoxon test). ***C***, Representative experiment showing rescue of persistent firing upon tonic depolarization of a neuron from a KO mouse. The first three pairs of voltage and current traces show that this neuron failed to fire persistently in response to increasing amounts of charge injection. In the fourth pair of traces (bottom), the neuron was tonically depolarized by 5 mV using a 50 pA constant current injection. The cell now fired persistently in response to a current pulse that initially failed to trigger persistent activity. Numbers to the left of current traces show size of tonic current. Calibration: 25 mV, 1 s, 400 pA. ***D***, Representative experiment from a wild-type mouse showing that tonic depolarization rescues persistent activity after pharmacological blockade of I_h. ***Di***, On the (*Figure legend continues*.)

polarizing current pulse (Fig. 6*C*). This persistent activity was robust and could last for as long as CCh was present in the bath or until the recording deteriorated (several tens of minutes). Some neurons failed to generate persistent activity even with very large and long depolarizations (800 pA for 8 s). The three groups of neurons—those that fired spontaneously, those that fired persistently in response to depolarization, and those that failed to fire persistently—were all mPFC layer V regular spiking pyramidal neurons and were otherwise indistinguishable electrophysiologically.

Does HCN1 contribute to the generation of CCh-induced intrinsic persistent activity? Although in the KO mice the depolarizing current steps were still able to elicit a burst of action potentials followed by a sADP (Fig. 6*D*), the fraction of neurons in which the sADP triggered persistent activity was much lower in the KO compared with control mice. Moreover, the probability of inducing persistent activity for a specific charge injection was significantly reduced (Fig. 6*E*,*F*). These data indicate that HCN1 and I_h promote the generation of CCh-induced intrinsic persistent firing states.

What mechanism underlies the effect of HCN1 on persistent activity?

Does HCN1 act as a pacemaker current to directly generate intrinsic persistent firing or does it act indirectly, for example, by influencing the resting potential or membrane resistance? As the sADP is thought to be the primary trigger of CCh-induced intrinsic persistent firing, we first determined the effect of HCN1 deletion on this slow afterdepolarization. We found that there was a reduction in the size of the sADP in the KO mice that was not caused by a change in excitability (i.e., the number of spikes generated during the stimulation; Fig. 7*A*). However, the decrease in the sADP alone is unlikely to explain the lack of intrinsic persistent activity as the probability of entering a persistently firing state for a given sized sADP was reduced for neurons from the KO mice relative to control littermates (Fig. 7*B*).

As the induction of CCh-induced intrinsic persistent activity has been found to be sensitive to changes in resting potential (Egorov et al., 2002; Tahvildari et al., 2007), we next examined whether the hyperpolarization of the resting membrane following HCN1 deletion was responsible for the deficit in persistent activity. By using constant current injection to shift the membrane potential in neurons from KO mice back to the range of the typical resting potential of control mice (on average a 5 mV depolarizing shift), we were able to rescue the induction of persistent activity ($n = 4$ out of 4; Fig. 7*C*). Tonic depolarization also rescued persistent firing in those neurons from control mice that initially failed to generate persistent firing ($n = 3$ out of 3).

The effect of HCN1 deletion to block intrinsic persistent activity is not caused by developmental effects or compensation

Even though HCN1 was deleted at a late developmental stage in our experiments (because of the late expression of Cre recombinase driven by the CaMKIIα promoter), it is possible that the effects on persistent activity are not directly caused by loss of HCN1 but may reflect some developmental or compensatory change. We therefore examined the effects of acute pharmacological blockade of I_h with ZD7288 (10 μM) in neurons from wild-type mice.

In the presence of the mixture of synaptic blockers and CCh, application of the organic I_h antagonist ZD7288 hyperpolarized the membrane, increased the input resistance, and abolished the membrane voltage sag in response to hyperpolarizing current steps, as expected from the blockade of I_h. In agreement with the KO results, acute inhibition of I_h also fully blocked the ability of the depolarizing pulse to trigger persistent activity ($n = 5$ of 5, data not shown).

To determine whether I_h was required for the maintenance as well as induction of persistent activity, we applied ZD7288 only after persistent firing had been established. We found that ZD7288 application invariably blocked ongoing persistent activity within minutes of its application at a dose that was sufficient to block I_h maximally ($n = 6$ of 6; Fig. 7*Di*). These pharmacological results are consistent with those obtained using the genetic ablation of HCN1 and support the conclusion that the presence of HCN1 and I_h is required for the efficient induction and maintenance of intrinsic persistent activity in layer V mPFC neurons.

Similar to our results with HCN1 deletion, the effect of pharmacological blockade of I_h to inhibit CCh-induced persistent firing results from a primary action to hyperpolarize the membrane. Thus, when ongoing persistent activity was blocked by ZD7288, persistent firing could be re-induced by a brief depolarizing current step provided that the hyperpolarizing action of I_h blockade was compensated by injection of a tonic depolarizing current ($n = 3$ out of 4; Fig. 7*D*). These results support the idea that HCN1 and I_h do not serve as primary pacemaker currents for the generation of persistent firing but instead modulate the ability of other conductances to generate persistent activity by shifting the resting potential to more positive voltages.

Role of HCN1 channels in the behavioral function of the PFC

The results described above demonstrate that deletion of HCN1 leads to profound alterations in the intrinsic properties of prefrontal neurons, causing deficits in their ability to generate CCh-induced intrinsic persistent activity as well as enhanced temporal summation of distal dendritic EPSPs. We next asked whether these physiological changes were correlated with any alterations in PFC-dependent behavior by testing the performance of HCN1 KO mice in spatial working memory and attention tasks. We found previously that forebrain-restricted HCN1 KO mice ($HCN1^{f/f,cre}$) have normal motor skills, sensory-motor gating, anxiety levels, and fear responses, ruling out any potential procedural or affective impediment that could hinder their performance in memory-based spatial tasks (Nolan et al., 2003, 2004).

Forebrain-restricted HCN1 KO mice and their control littermates were trained on a DNMP task using an 8-arm radial maze. In this task, mice retrieved a food reward from a single open arm of the maze. After a variable delay period the mice were returned to the maze and presented with a choice between the original

←

(*Figure legend continued.*) left is shown an example recording of the reduction of I_h in response to 0.7 and 50 μM ZD7288 (−50 to −100 mV, 2 s step). On the right is the average concentration-dependent blockade with two additional doses (right; $n = 2$–5 per point). The red trace is a Hill curve fit (IC_{50} of 1.1 μM indicated). ***Dii***, Example of current-clamp recording showing the responses of a control layer V neurons to two current pulses that were subthreshold and suprathreshold for triggering persistent firing (current injection commands are indicated below the voltage traces). ***Diii***, Bath-applied ZD7288 at 10 μM, which we found to have a maximal blocking effect on I_h (see ***Di***), halted persistent firing within a few minutes of application (the average time taken to stop firing was 5 min in 6 experiments). The first voltage trace shows the transition from persistent firing to silence, while the second trace shows the stable, silent, and hyperpolarized membrane potential (relative to control conditions) in the presence of ZD7288. In the last trace, the membrane was brought back to its initial resting potential using tonic current injection. A depolarizing current pulse now induced persistent firing, while I_h was fully blocked by ZD7288. Calibration: 25 mV, 1 s, 400 pA.

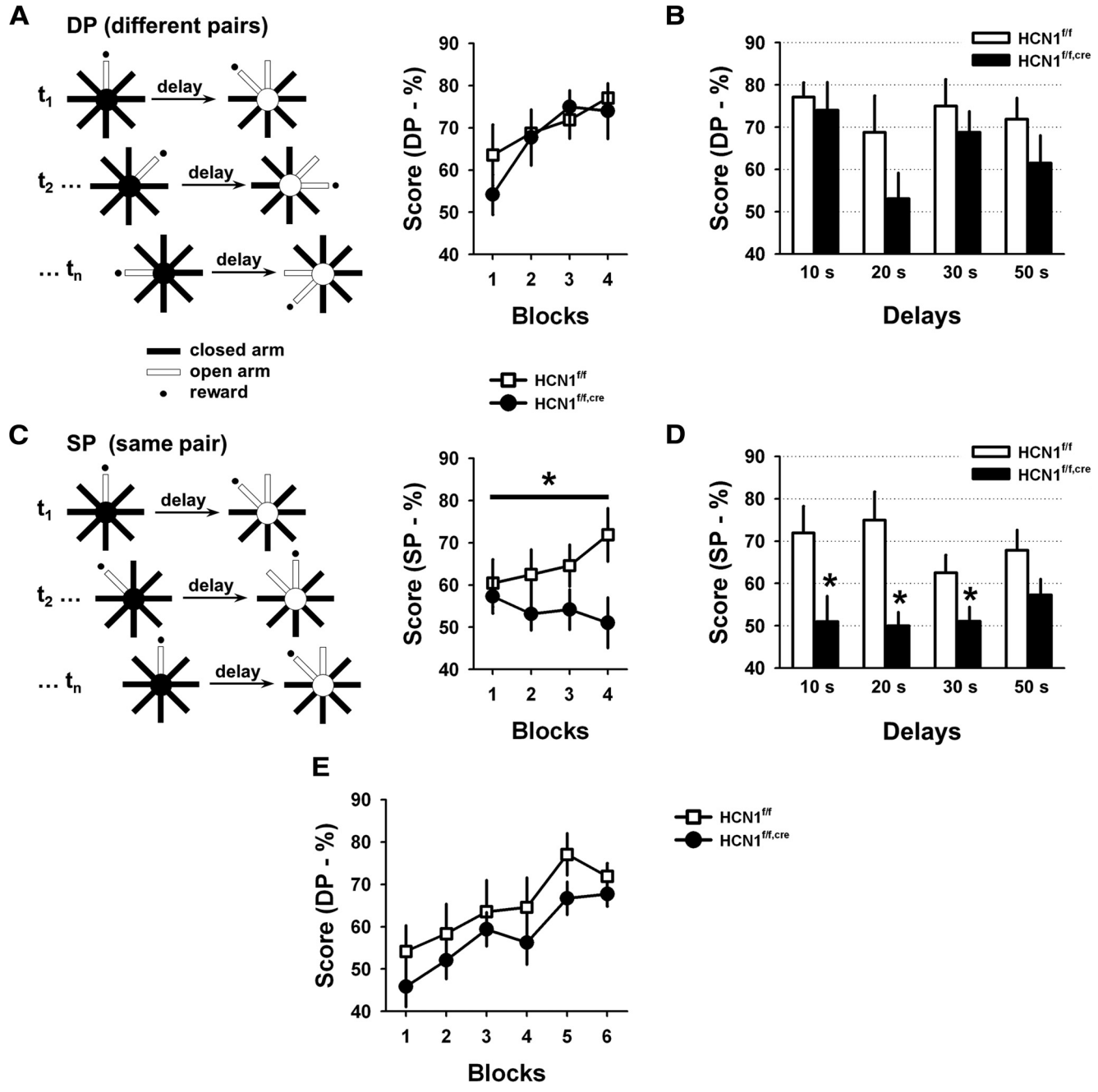

Figure 8. Impact of HCN1 deletion on spatial working memory. ***A***, Performance of control and KO mice ($n = 8$) in the standard version of the DNMP task in the 8-arm radial maze. Left, Diagram depicting the task. On each consecutive trial ($t_1, t_2, \ldots, t_n$) two distinct pairs of arms were used (DP). Right, Average performance during successive 2 d blocks in the training phase of the task using a 10 s delay (□, control; ●, KO). Each block shows the mean performance during 2 d of training consisting of six trials per day. ***B***, Plot of the mean performance of the control (open bars) and KO (filled bars) animals in the standard version of the task (DP), when animals were tested using several delay intervals. There was no significant difference in performance between genotypes. ***C***, Performance of the mice in the modified version of the task in which the same pair of arms (SP) was used in every trial. Left, Diagram depicting the modified task. Right, Average score during the training phase with a 10 s delay (□, control; ●, KO). KO mice showed a significant deficit in performance in this task (two-way ANOVA with repeated measures; $p < 0.03$, effect of genotype; $n = 8$ in each group). ***D***, Plot of mean performance in the SP version of the task following training when mice were tested using different delay periods. The performance of the KO mice was significantly lower than that of control mice at delays of 10, 20, and 30 s (10 s delay: $p < 0.04$; 20 s delay: $p < 0.01$; 30 s delay: $p < 0.05$; 50 s delay: $p > 0.1$; all unpaired t test, $n = 8$ in each group). ***E***, HCN1 $^{f/f,cre}$ KO mice perform at a level comparable to HCN1 $^{f/f}$ control littermates when tested on the standard (DP) version of the delayed non-match to place task following initial testing on the modified (SP) version of the task, in which they do show a deficit (***C***, ***D***). The final level of performance after six blocks of training was similar to that obtained when mice were tested initially with this version of the task.

open arm and an adjacent open arm, which now contained the food reward. Thus the mice had to remember the location of the original open arm so they could correctly choose the newly opened one to obtain a reward. In the standard version of the task, different pairs of arms were used in each consecutive trial (Fig. 8*A*, DP, different pairs). In a modified version of this task the same pair of arms were used on every trial, with the initial food reward randomly assigned to one of the arms (Fig. 8*C*, SP, same pair). This modified version of the task places a stronger load on the executive function of PFC as the memory of the previous goal arm can interfere with the choice during subsequent trials, a phenomenon known as proactive interference. Such interference oc-

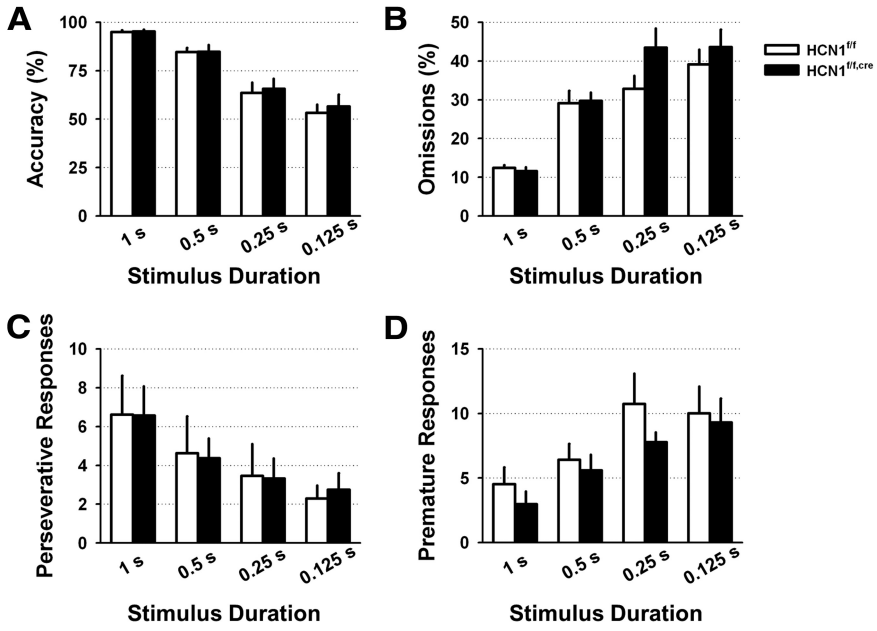

Figure 9. Deletion of HCN1 does not alter attentional performance in the 5-CSRT task. Control and HCN1 KO animals were tested with variable stimulus durations ranging from 1 s to 0.125 s. Their performance was assessed by measuring: their accuracy defined as the percentage of correct responses from the total number of responses (correct plus incorrect) (***A***); the percentage of trials in which they did not respond (omissions) (***B***); the number of repeated responses they made in immediate succession (perseverative responses) (***C***); and the number of premature responses (***D***). None of these parameters differed significantly between control and KO animals.

curs when memories are formed in similar contexts and is large if memorized items are closely related to each other, which is the case in the SP task. The resolution of interference belongs to a set of executive functions recruited during working memory tasks and is thought, like many other executive functions, to involve the PFC (D'Esposito et al., 1995, 1999; Fuster, 2001; Kane and Engle, 2002; Baddeley, 2003; Jonides and Nee, 2006; Postle, 2006).

The behavioral performance of HCN1$^{f/f}$ and HCN1$^{f/f,cre}$ littermates was similar in the standard version of the DNMP during training and with prolonged delays (Fig. 8*A*,*B*). However, when switched to the modified version of the task with heightened interference (instead of distinct pairs of arms, the same pairs of arms were used in consecutive trials; see Material and Methods), the HCN1 KO mice displayed a marked deficit in performance compared with their control littermates (Fig. 8*C*), with significantly lower scores compared with control mice at 10, 20, and 30 s delays (Fig. 8*D*). This deficit was not due to learning fatigue with extended training as the KO mice performed comparably to control littermates when they were retrained on the standard version of the task following testing on the modified task (Fig. 8*E*). In addition, this deficit is unlikely to result from a loss in vigilance or attention, as the KO mice performed as well as controls in a standard attentional task, the 5-choice serial reaction time task (5-CSRT; Bari et al., 2008; Fig. 9). Thus, these observations suggest that the loss of HCN1 weakens the resolution of proactive interference during working memory.

Several additional results support the view that the decreased performance reflects a role of HCN1 in the resolution of proactive interference. First, the performance of the KO animals on the first trial of an SP session, which by definition is not prone to interference, was higher than the composite score on subsequent trials, that is, when interference starts to be active (trial 1 vs trial 2–6; 68.8 ± 6.7% vs 50.6 ± 3.0%; $p = 0.029$; $n = 8$; 10 s delay). In contrast, there was no statistically significant difference in the control mice between these groups of trials (73.4 ± 9.3% vs 63.1 ± 3.1%; $p = 0.26$). Second, interference should be at its peak when the past memory is in greatest conflict with the present choice. In the DNMP task this greatest conflict will occur when consecutive trials require an alternation of choices (e.g., when arm A should be chosen in trial $n - 1$ and arm B should be chosen in trial n; Fig. 10*A*) and when the memory of the first choice was reinforced (that is, when the mouse correctly chose arm A on trial $n - 1$). Consistent with a deficit in interference resolution, we found that the performance of KO mice in 10 s delay trials with such peak interference was lower than their average performance in this task (Fig. 10*C*). In contrast, this effect was absent in the control animals, suggesting that their resolution of proactive interference was intact, active, and strong (Fig. 10*B*). Interestingly, a study in rats previously found that the impact of interference on working memory performance, in a task similar to ours and with similar delays, can only be revealed by lesions of the PFC, suggesting that normal animals are equipped with the means to fully resist interference, at least in the tasks used in the two studies (Porter and Mair, 1997). Altogether, these results support the idea that the working memory deficit observed in the forebrain-restricted HCN1 KO mice is directly linked to a diminished ability to resolve proactive interference during the use of working memory. However, as HCN1 was deleted throughout the forebrain, these experiments do not allow us to conclude that the behavioral deficit is specifically caused by the loss of HCN1 in PFC.

Prefrontal deletion of HCN1 is sufficient to alter the resolution of interference during working memory

To explore the importance of HCN1 selectively in mPFC for resolution of interference, we restricted HCN1 deletion to this brain region by injecting lentiviral vectors expressing Cre recombinase under the control of the CaMKIIα promoter (LV-Cre) into the mPFC of homozygous HCN1 floxed mice (HCN1$^{f/f}$). We first tested the feasibility of this approach by injecting mice with LV-Cre in one hemisphere and LV-GFP in the other. Two months after injection the mice were killed and the expression of HCN1 was analyzed in fixed brain slices. We found that LV-Cre expression in the PFC led to a dramatic, highly localized deletion of HCN1 (Fig. 11*A*,*B*). Whole-cell recordings of electrophysiological properties of layer V neurons confirmed the efficacy of virally expressed Cre in deleting HCN1. Thus Cre-positive neurons were found to have a significant reduction in I_h and alteration of membrane properties similar to those observed in the KO mice (Fig. 11*C*,*D*), including the reduction in the ability to generate intrinsic persistent firing (Fig. 11*E*,*F*).

To determine whether the restricted deletion of HCN1 from mPFC was sufficient to impair working memory performance, we compared the behavior of three groups of HCN1$^{f/f}$ littermates on the radial maze DNMP task: an experimental group bilaterally injected in mPFC with LV-Cre to delete HCN1, a control group of mice injected in mPFC with lentivirus-expressing GFP (LV-GFP), and a second unoperated control group (no viral injection). Because there

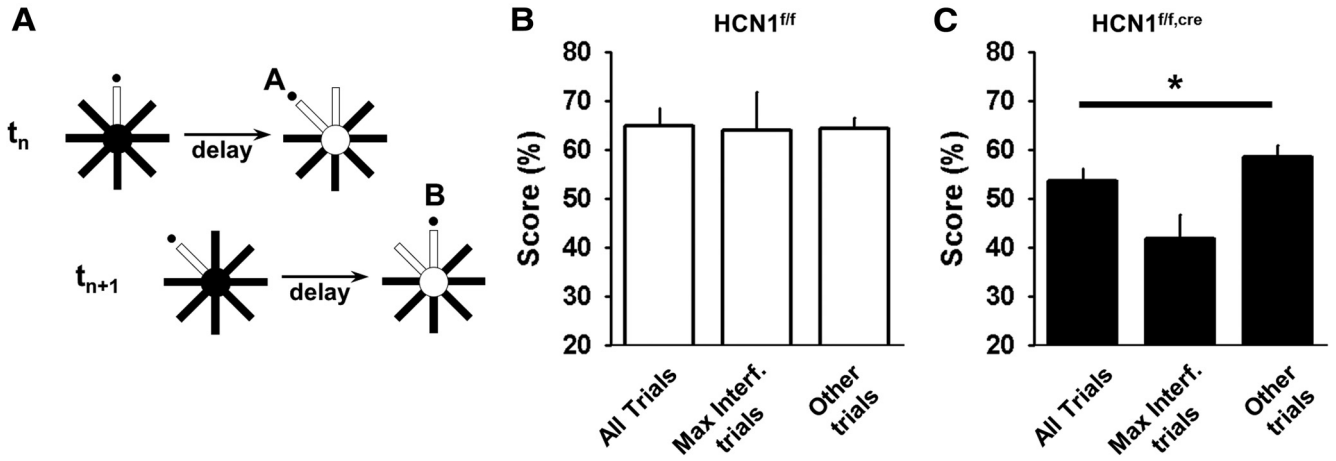

Figure 10. Proactive interference is impaired in the HCN1 $^{f/f,cre}$ forebrain KO mice. ***A***, Example of a maximal interference trial sequence. A trial (t_{n+1}) has the greatest potential for interference when the previous trial (t_n) had an alternate goal that was rewarded. ***B***, ***C***, Average performance of control (***B***) and KO mice (***C***) on the second trial of maximal interference sequences (Max. Interf. trials) compared with their performance on all trials (All trials), or only the subset of trials that were distinct from the Max. Interf. trials (Other trials). $p < 0.01$ for the KO group, one-way ANOVA; four blocks with 10 s delay; $n = 8$ in each group.

was no significant difference in the scores of the two control groups, these populations were combined for the analysis.

Similar to what we observed with the forebrain-restricted HCN1 KO, we found no difference between the mPFC LV-CRE KO mice and the two control groups in the standard version of the working memory task (Fig. 12*A*). However, when the mice were tested on the modified version of the task with increased interference, the prefrontal-restricted KO animals exhibited once again a clear deficit in performance compared with either the GFP control group or the combined control group (GFP-injected and unoperated mice) with delays of 10 and 20 s (Figs. 12*B*). In addition, performance of the mPFC-restricted KO mice on trials with peak interference showed a greater impairment compared with their average performance on all trials (Fig. 12*C*), similar to what we observed in the forebrain KO mice. As further support for an impaired resolution of interference, the performance of the LV-Cre-injected animals on the first trial of a session was higher than the composite score on subsequent trials (trial 1 vs trial 2–6; 68.9 ± 4.0% vs 58.0 ± 2.2%; $p = 0.01$; $n = 15$; 10 s delay); an effect that is comparable to that observed in the forebrain KO mouse. The somewhat smaller performance deficits seen with mPFC-restricted HCN1 deletion compared with forebrain-restricted deletion could indicate a role for other brain regions, such as hippocampus, or the fact that the viral vector infected only a fraction of mPFC neurons.

After the behavioral testing ended, we verified correct location of expression of GFP or Cre and the efficient deletion of HCN1 in the PFC of the animals used for behavioral testing using immunocytochemistry (Fig. 12*D*,*E*). These results provide strong evidence that a selective alteration in PFC function through local deletion of HCN1 is largely responsible for the behavioral deficit in the DNMP working memory task seen in the forebrain-restricted KO mice.

Discussion

HCN1 enables intrinsic persistent firing in PFC neurons

Using spatially restricted gene deletion in mice, we found that HCN1-containing channels make an important contribution to intrinsic persistent firing of layer V prefrontal pyramidal neurons and to the behavioral output of the PFC. At the cellular level, HCN1 deletion induced a substantial loss of I_h, which altered the intrinsic and integrative properties of these neurons and shifted the resting potential to more negative voltages. The hyperpolarization, in turn, hindered the induction of persistent firing in these neurons. In contrast, deletion of HCN1 had little effect on the duration or frequency of synaptic network-dependent up states or on the ability of these neurons to undergo LTP. Thus, our results established a correlation between a deficit in prefrontal-dependent working memory behavior and a loss in the ability of cortical neurons to generate intrinsic persistent firing and an increase in temporal summation of distal dendritic EPSPs. Although this correlation is intriguing, it is important to emphasize that our experiments do not allow us to establish whether there is a causal relationship between the altered electrophysiological properties of layer V mPFC neurons with the decreased executive function.

Previous studies have investigated the role of I_h and HCN1 in persistent firing in PFC with conflicting results. Winograd et al. (2008) found that persistent firing could be triggered in a minority of spontaneously active PFC neurons in ferret and guinea pig following hyperpolarizing pulses. Although they implicated I_h in this effect, they used extremely high concentrations of ZD7288 that are known to exert nonspecific actions (Chevaleyre and Castillo, 2002; Felix et al., 2003; Chen, 2004; Sánchez-Alonso et al., 2008). Challenging the idea that I_h is necessary for persistent firing, Wang et al. (2007) examined persistent firing in ferret slices and monkey PFC neurons *in vivo*, and concluded that I_h and HCN1 actually inhibit persistent firing. These data again relied on a pharmacological blockade of I_h using high concentrations or ZD7288 *in vitro* and unknown concentrations of various pharmacological agents *in vivo*. In addition, this study also reported that HCN1 knockdown with siRNA enhanced working memory performance in mice, causing these authors to propose that HCN1 acts as an inhibitory constraint of PFC-dependent persistent firing and working memory behavior.

Prefrontal HCN1 channels support the resolution of proactive interference during working memory

We find that deletion of HCN1 from PFC neurons has distinct consequences on the ability of mice to perform two related working memory tasks. There was no impairment in the ability of mice

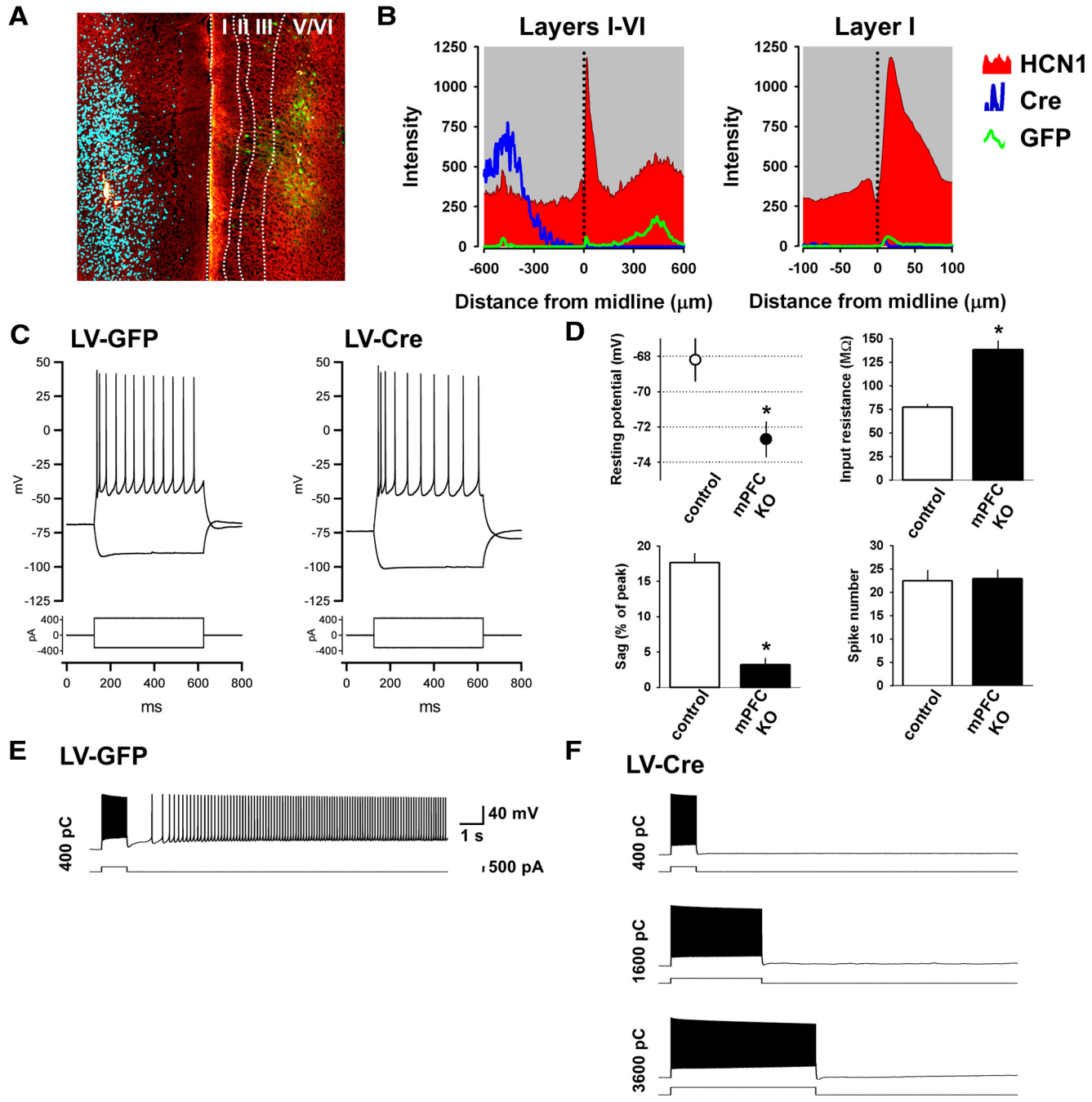

Figure 11. Virally mediated deletion of HCN1 from medial prefrontal neurons recapitulates the deficits in intrinsic persistent activity observed in prefrontal neurons of forebrain-restricted HCN1 KO mice. ***A***, Confocal micrograph of mPFC in fixed coronal slice from an HCN1 $^{f/f}$ animal injected with lentivirus-expressing Cre (LV-Cre) in the left hemisphere and lentivirus-expressing GFP (LV-GFP) in the right hemisphere. Staining shown for HCN1 (red/yellow), Cre (cyan), and GFP (green). There was a dramatic reduction in HCN1 signal on the side expressing Cre (left) compared with contralateral side expressing GFP (right). ***B***, Quantification of staining intensity across the thickness of PFC (left). Expanded view of signal in layer I (right), where HCN1 is enriched. Note the asymmetric distribution of HCN1 across the midline (dotted line). ***C***, Examples of membrane potential responses to depolarizing and hyperpolarizing steps in a control LV-GFP-infected neuron (left) and an HCN1-KO, LV-Cre-infected neuron (right). ***D***, Comparison of the intrinsic membrane properties of neurons from control (green neurons from HCN1 $^{f/f}$ + LV-GFP-injected slices, $n = 5$; and nonfluorescent neurons from the HCN1 $^{f/f}$ + LV-Cre + AAV-flex-GFP-injected slices, $n = 5$) and KO groups (green neurons from HCN1 $^{f/f}$ + LV-Cre + AAV-flex-GFP-injected slices, $n = 11$). The resting membrane was more hyperpolarized ($p < 0.01$, unpaired t test), the input resistance larger (measured near rest, $p < 0.0001$, unpaired t test), the voltage sag in response to a −400 pA, 1 s step smaller ($p < 0.0000001$, unpaired t test), and the spike response to a 400 pA, 1 s step unaltered in the KO group versus the control group. ***E***, Example of CCh-induced intrinsic persistent activity in a neuron infected with LV-GFP. In the control group, persistent activity could be triggered in 86% of HCN1-expressing neurons ($n = 7$). ***F***, Example of an LV-Cre-infected neuron in an HCN1 $^{f/f}$ mouse refractory to the induction of persistent activity. In the KO group, persistent activity could only be induced in 40% of the Cre-expressing neurons ($n = 10$). Same scale as in ***C***. Charge injected indicated on the left side of each representative trace.

to perform a delayed non-match to place task in an 8-arm radial maze that required the animals to retain information over the short term. In contrast, there was a marked deficit in the performance of a version of the task in which proactive interference was prominent. Interestingly, the effect of HCN1 deletion was seen only when the task featured a short delay of 30 s or less, perhaps because longer time intervals are detrimental to interference processes. This is also in agreement with a previous study using a similar task that found that the mPFC was only recruited with short delays (Lee and Kesner, 2003).

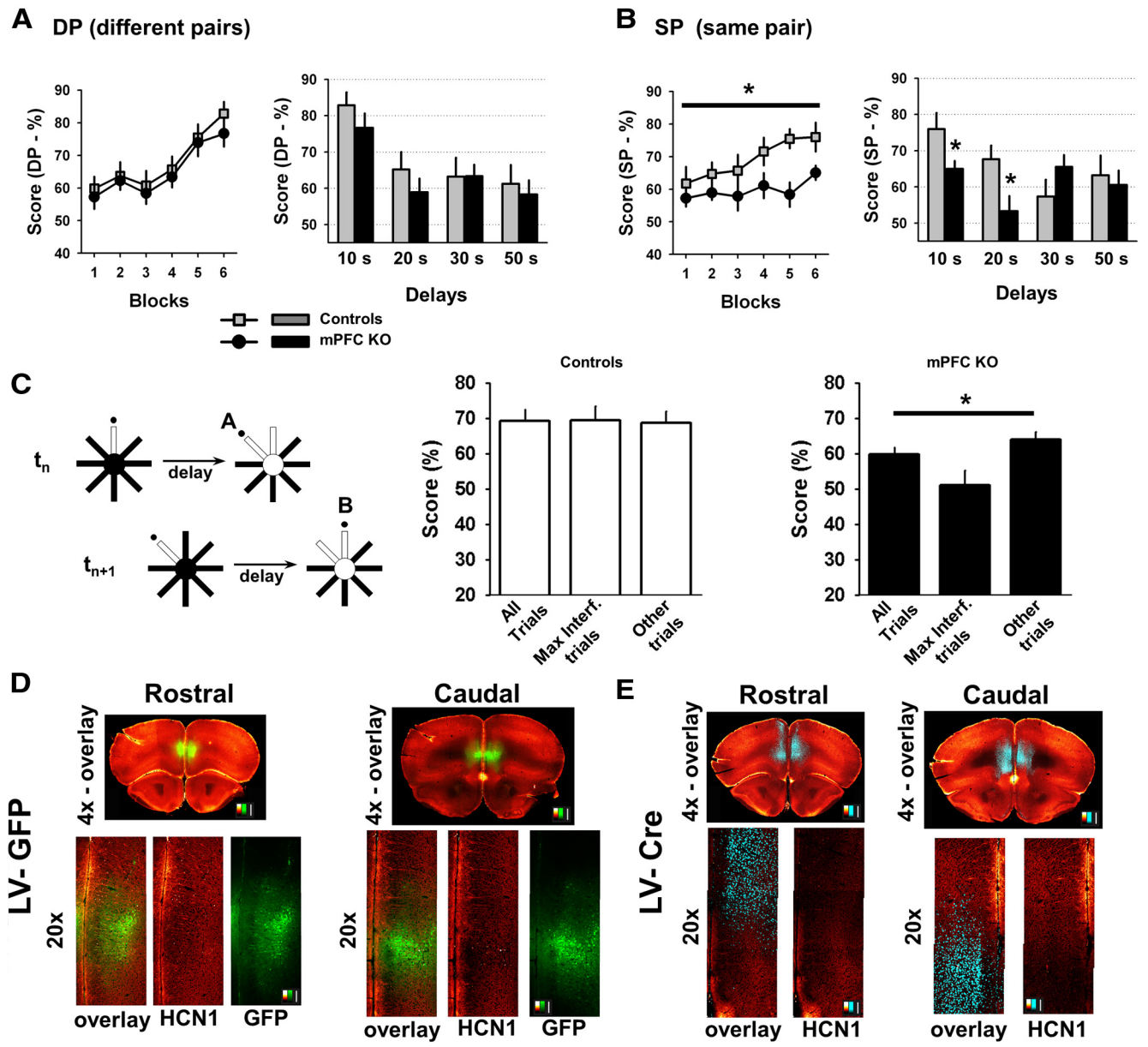

Figure 12. Virally mediated deletion of HCN1 in mPFC is sufficient to impair performance in the DNMP task with heightened interference. ***A***, Performance of control mice versus mice with a deletion of HCN1 restricted to mPFC in the standard version of the DNMP task (DP). Control mice: HCN1$^{f/f}$ mice ($n = 8$) and HCN1$^{f/f}$ mice injected in mPFC with lentivirus-expressing GFP (HCN1$^{f/f}$+LV-GFP; $n = 9$). mPFC KO mice: HCN1$^{f/f}$ mice injected in mPFC with lentivirus-expressing Cre recombinase (HCN1$^{f/f}$+LV-Cre; $n = 15$). Left, Average score during the training phase with a 10 s delay (control, gray squares; mPFC KO, ●). Right, Mean performance across several intratrial delays for control (gray bars) and mPFC KO (black bars) mice. There was no significant difference in performance between genotypes. ***B***, Performance of the same animals in the modified version of the task (SP). Left, Average score during training phase using 10 s delay. mPFC KO group exhibits a significant deficit relative to control (two-way ANOVA with repeated measures, $p < 0.03$, comparing controls to mPFC KO, $n = 17$ and 15, respectively). Right, Mean performance in the SP version of the task following training with mice tested using different delays. The performance of the HCN1$^{f/f}$+LV-Cre group was significantly lower than that of the combined control group for delays of 10 s ($p < 0.05$, unpaired t test) and 20 s ($p < 0.02$, unpaired t test). ***C***, Average performance of control (middle) and mPFC KO mice (right) on maximal interference trials (Max. Interf. Trials as in trial sequence depicted on far left) compared with their performance on all trials (All trials) or subset of trials distinct from Max. Int. trials (Other trials). One-way ANOVA $p < 0.02$ for the KO group; six blocks with 10 s delay ($n = 15$). ***D***, Immunofluorescence images of HCN1 and GFP in coronal brain slices from a control HCN1$^{f/f}$ mouse injected with LV-GFP. Coronal slices shown from the rostral (left) and caudal (right) parts of the PFC (red/yellow look up table; LUT: HCN1 signal; green LUT: GFP signal). Higher magnification images (20×) centered on the mPFC are presented below; detection channels are either superimposed (overlay) or presented separately (HCN1 and GFP). Scale bars: 500 μm for the full slice, 100 μm for the higher magnification. ***E***, Similar images but for tissue obtained from an HCN1$^{f/f}$ animal injected with LV-Cre (red/yellow LUT: HCN1; cyan LUT: Cre immunofluorescence). Scale bars: 500 μm, top images; 100 μm bottom images. Note loss of HCN1 signal, which is particularly apparent in layer I in regions in which deep layer neurons express Cre.

At first glance, our results appear contradictory with earlier behavioral results from Wang et al. (2007). This previous study reported that iontophoretic injection of submicromolar concentrations of ZD7288 (which we find to have minimal effects on I_h in mice; Fig. 7*Di*) or viral expression of siRNA to knockdown HCN1 in PFC resulted in an improved performance of rats in a T-maze task (Wang et al., 2007). However, higher concentrations of ZD7288, in the range needed to produce the substantial reductions in I_h that we have examined here, did not increase working memory performance. This latter finding is consistent with our observation that prefrontal HCN1 channels are not required for optimal working

memory performance in conditions with minimal interference (a parameter not controlled by the paradigm used by Wang et al., 2007). At present it is not clear how weak inhibition of I_h enhances persistent firing or working memory performance.

Another puzzling set of results from Wang et al. (2007) concerns the action of Rp-cAMPS. Whereas Rp-cAMPs acts as an antagonist of cAMP by blocking activation of protein kinase A, it also acts as an agonist for I_h (Ingram and Williams, 1996; Bois et al., 1997). Thus the findings that iontophoretic injections of either ZD7288 or Rp-cAMPS similarly enhance persistent firing in monkey PFC (Wang et al., 2007) and that Rp-cAMPS enhances working memory performance in rats (Ramos et al., 2003) suggest that I_h and HCN1 may not necessarily suppress working memory performance under all conditions.

Our finding that HCN1 channels in the PFC may contribute to performance of certain executive functions associated with working memory (i.e., the resolution of interference), as opposed to simple memory storage per se, is in agreement with several previous findings on PFC function. First, an earlier study in rats using a paradigm very similar to ours (Porter and Mair, 1997) reported that lesions of the PFC spare performance in the DP task but cause a deficit in the SP task. In the same experiments, We also found that normal animals displayed similar levels of performance in these two tasks, which suggests that under normal conditions the PFC effectively opposes proactive interference. The similarity of our findings using genetic perturbations with this previous lesion study supports our interpretation that prefrontal HCN1 channels are important for the resolution of proactive interference during working memory. Second, various studies in humans have also suggested that the PFC plays a crucial role in the resolution of proactive interference in working memory (Jonides and Nee, 2006). Third, the occurrence of sustained activity in PFC neurons has been linked to processes other than simple short-term memory maintenance, such as resistance to interference, attentional selection, information processing, response preparation, or integration of affect (D'Esposito et al., 1995; Miller et al., 1996; Watanabe, 1996; Rowe et al., 2000; Bor et al., 2003; Gray et al., 2003; Lebedev et al., 2004; Postle, 2006).

Overall, our analysis strongly suggests that prefrontal HCN1 channels contribute to the resolution of proactive interference during working memory and highlight, in mice, a role for the PFC in the implementation of this executive function.

Cellular versus network mechanisms of persistent firing and their role in different functions of the PFC

Our findings are consistent with the idea that HCN1 facilitates PFC function by acting on intrinsic neuronal properties that are important for generating a nonsynaptic form of persistent activity. Interestingly, the cellular mechanisms of intrinsic persistent activity and the behavioral output of the PFC share a dependence on the activation of muscarinic ACh receptors (Spencer et al., 1985; Granon et al., 1995; Grasby et al., 1995; Wall and Messier, 2001; Anagnostaras et al., 2003; Chudasama et al., 2004; Seeger et al., 2004). In addition, muscarinic receptors can shape the temporal dynamics of neocortical activity *in vivo*, including during periods of sustained firing (Rigdon and Pirch, 1984; Buzsaki et al., 1988; Metherate et al., 1992; Steriade et al., 1993a; Goard and Dan, 2009). When combined with these results, our observations suggest a close functional relationship between the mechanisms of intrinsic persistent firing and the prefrontal processes that influence working memory behavior. However, it is important to note that our study, similar to other genetic approaches, cannot prove a causal link between persistent activity and behavior. It will therefore be important for future studies to explore further the idea that intrinsic persistent firing is an important neural mechanism for the executive functions mediated by the PFC.

Finally, it is interesting to note that reverberatory circuit mechanisms associated with up and down states do not require HCN1 (Fig. 5), and are thus unlikely to be responsible for the deficit in resolution of interference in the KO mice. This result appears to differ from results obtained in ferret slices that showed that application of 50 μM ZD7288 increased the duration of up states (Wang et al., 2007). However, such a high concentration of the I_h blocker is likely to result in off-target effects, as previously described (Chevaleyre and Castillo, 2002; Felix et al., 2003; Chen, 2004; Sánchez-Alonso et al., 2008). Regardless, the absence of effect on up and down states in the HCN1 KO mice suggests that neural activity generated by recurrent network architectures may be more important for the actual maintenance of information in working memory, an ability that appears intact following deletion of HCN1. Thus, distinct intrinsic and extrinsic mechanisms for persistent activity may coexist in the same cells and in the same circuits to fulfill distinct roles in the circuit dynamics that mediate the diverse contributions of PFC to behavior.

References

Anagnostaras SG, Murphy GG, Hamilton SE, Mitchell SL, Rahnama NP, Nathanson NM, Silva AJ (2003) Selective cognitive dysfunction in acetylcholine M1 muscarinic receptor mutant mice. Nat Neurosci 6:51–58. CrossRef Medline

Andrade R (1991) Cell excitation enhances muscarinic cholinergic responses in rat association cortex. Brain Res 548:81–93. CrossRef Medline

Atkinson SE, Williams SR (2009) Postnatal development of dendritic synaptic integration in rat neocortical pyramidal neurons. J Neurophysiol 102:735–751. CrossRef Medline

Baddeley A (2003) Working memory: looking back and looking forward. Nat Rev Neurosci 4:829–839. CrossRef Medline

Baeg EH, Kim YB, Huh K, Mook-Jung I, Kim HT, Jung MW (2003) Dynamics of population code for working memory in the prefrontal cortex. Neuron 40:177–188. CrossRef Medline

Bari A, Dalley JW, Robbins TW (2008) The application of the 5-choice serial reaction time task for the assessment of visual attentional processes and impulse control in rats. Nat Protoc 3:759–767. CrossRef Medline

Bois P, Renaudon B, Baruscotti M, Lenfant J, DiFrancesco D (1997) Activation of f-channels by cAMP analogues in macropatches from rabbit sinoatrial node myocytes. J Physiol 501:565–571. CrossRef Medline

Bor D, Duncan J, Wiseman RJ, Owen AM (2003) Encoding strategies dissociate prefrontal activity from working memory demand. Neuron 37:361–367. CrossRef Medline

Buzsaki G, Bickford RG, Ponomareff G, Thal LJ, Mandel R, Gage FH (1988) Nucleus basalis and thalamic control of neocortical activity in the freely moving rat. J Neurosci 8:4007–4026. Medline

Chen C (2004) ZD7288 inhibits postsynaptic glutamate receptor-mediated responses at hippocampal perforant path-granule cell synapses. Eur J Neurosci 19:643–649. CrossRef Medline

Chen X, Sirois JE, Lei Q, Talley EM, Lynch C 3rd, Bayliss DA (2005) HCN subunit-specific and cAMP-modulated effects of anesthetics on neuronal pacemaker currents. J Neurosci 25:5803–5814. CrossRef Medline

Chen X, Shu S, Bayliss DA (2009) HCN1 channel subunits are a molecular substrate for hypnotic actions of ketamine. J Neurosci 29:600–609. CrossRef Medline

Chevaleyre V, Castillo PE (2002) Assessing the role of Ih channels in synaptic transmission and mossy fiber LTP. Proc Natl Acad Sci U S A 99:9538–9543. CrossRef Medline

Chudasama Y, Dalley JW, Nathwani F, Bouger P, Robbins TW (2004) Cholinergic modulation of visual attention and working memory: dissociable effects of basal forebrain 192-IgG-saporin lesions and intraprefrontal infusions of scopolamine. Learn Mem 11:78–86. CrossRef Medline

Compte A (2006) Computational and in vitro studies of persistent activity: edging towards cellular and synaptic mechanisms of working memory. Neuroscience 139:135–151. CrossRef Medline

Cossart R, Aronov D, Yuste R (2003) Attractor dynamics of network UP states in the neocortex. Nature 423:283–288. CrossRef Medline

Crunelli V, Hughes SW (2010) The slow (<1 Hz) rhythm of non-REM sleep: a dialogue between three cardinal oscillators. Nat Neurosci 13:9–17. CrossRef Medline

Day M, Carr DB, Ulrich S, Ilijic E, Tkatch T, Surmeier DJ (2005) Dendritic excitability of mouse frontal cortex pyramidal neurons is shaped by the interaction among HCN, Kir2, and Kleak channels. J Neurosci 25:8776–8787. CrossRef Medline

Dégenètais E, Thierry AM, Glowinski J, Gioanni Y (2002) Electrophysiological properties of pyramidal neurons in the rat prefrontal cortex: an in vivo intracellular recording study. Cereb Cortex 12:1–16. CrossRef Medline

Dembrow NC, Chitwood RA, Johnston D (2010) Projection-specific neuromodulation of medial prefrontal cortex neurons. J Neurosci 30:16922–16937. CrossRef Medline

Derjean D, Bertrand S, Nagy F, Shefchyk SJ (2005) Plateau potentials and membrane oscillations in parasympathetic preganglionic neurones and intermediolateral neurones in the rat lumbosacral spinal cord. J Physiol 563:583–596. Medline

D'Esposito M, Detre JA, Alsop DC, Shin RK, Atlas S, Grossman M (1995) The neural basis of the central executive system of working memory. Nature 378:279–281. CrossRef Medline

D'Esposito M, Postle BR, Jonides J, Smith EE (1999) The neural substrate and temporal dynamics of interference effects in working memory as revealed by event-related functional MRI. Proc Natl Acad Sci U S A 96:7514–7519. CrossRef Medline

Dittgen T, Nimmerjahn A, Komai S, Licznerski P, Waters J, Margrie TW, Helmchen F, Denk W, Brecht M, Osten P (2004) Lentivirus-based genetic manipulations of cortical neurons and their optical and electrophysiological monitoring in vivo. Proc Natl Acad Sci U S A 101:18206–18211. CrossRef Medline

Dull T, Zufferey R, Kelly M, Mandel RJ, Nguyen M, Trono D, Naldini L (1998) A third-generation lentivirus vector with a conditional packaging system. J Virol 72:8463–8471. Medline

Egorov AV, Hamam BN, Fransén E, Hasselmo ME, Alonso AA (2002) Graded persistent activity in entorhinal cortex neurons. Nature 420:173–178. CrossRef Medline

Felix R, Sandoval A, Sánchez D, Gómora JC, De la Vega-Beltrán, JL, Treviño CL, Darszon A (2003) ZD7288 inhibits low-threshold Ca2+ channel activity and regulates sperm function. Biochemical and biophysical research communications 311:187–192. CrossRef Medline

Fransén E, Tahvildari B, Egorov AV, Hasselmo ME, Alonso AA (2006) Mechanism of graded persistent cellular activity of entorhinal cortex layer v neurons. Neuron 49:735–746. CrossRef Medline

Funahashi S, Bruce CJ, Goldman-Rakic PS (1989) Mnemonic coding of visual space in the monkey's dorsolateral prefrontal cortex. J Neurophysiol 61:331–349. Medline

Fuster JM (2001) The prefrontal cortex–an update: time is of the essence. Neuron 30:319–333. CrossRef Medline

Fuster JM, Alexander GE (1971) Neuron activity related to short-term memory. Science 173:652–654. CrossRef Medline

Goard M, Dan Y (2009) Basal forebrain activation enhances cortical coding of natural scenes. Nat Neurosci 12:1444–1449. CrossRef Medline

Goldman-Rakic PS (1995) Cellular basis of working memory. Neuron 14:477–485. CrossRef Medline

Granon S, Poucet B, Thinus-Blanc C, Changeux JP, Vidal C (1995) Nicotinic and muscarinic receptors in the rat prefrontal cortex: differential roles in working memory, response selection and effortful processing. Psychopharmacology 119:139–144. CrossRef Medline

Grasby PM, Frith CD, Paulesu E, Friston KJ, Frackowiak RS, Dolan RJ (1995) The effect of the muscarinic antagonist scopolamine on regional cerebral blood flow during the performance of a memory task. Exp Brain Res 104:337–348. Medline

Gray JR, Chabris CF, Braver TS (2003) Neural mechanisms of general fluid intelligence. Nat Neurosci 6:316–322. CrossRef Medline

Haider B McCormick DA (2009) Rapid neocortical dynamics: cellular and network mechanisms. Neuron 62:171–189. CrossRef Medline

Haj-Dahmane S, Andrade R (1996) Muscarinic activation of a voltage-dependent cation nonselective current in rat association cortex. J Neurosci 16:3848–3861. Medline

Haj-Dahmane S, Andrade R (1998) Ionic mechanism of the slow afterdepolarization induced by muscarinic receptor activation in rat prefrontal cortex. J Neurophysiol 80:1197–1210. Medline

Ingram SL Williams JT (1996) Modulation of the hyperpolarization-activated current (Ih) by cyclic nucleotides in guinea-pig primary afferent neurons. J Physiol 492:97–106. Medline

Jonides J, Nee DE (2006) Brain mechanisms of proactive interference in working memory. Neuroscience 139:181–193. CrossRef Medline

Jonides J, Lewis RL, Nee DE, Lustig CA, Berman MG, Moore KS (2008) The mind and brain of short-term memory. Annu Rev Psychol 59:193–224. CrossRef Medline

Jung MW, Qin Y, McNaughton BL, Barnes CA (1998) Firing characteristics of deep layer neurons in prefrontal cortex in rats performing spatial working memory tasks. Cereb Cortex 8:437–450. CrossRef Medline

Kane MJ, Engle RW (2002) The role of prefrontal cortex in working-memory capacity, executive attention, and general fluid intelligence: an individual-differences perspective. Psychon Bull Rev 9:637–671. CrossRef Medline

Kiehn O (1991) Plateau potentials and active integration in the 'final common pathway' for motor behaviour. Trends Neurosci 14:68–73. CrossRef Medline

Lavin A, Grace AA (2001) Stimulation of D1-type dopamine receptors enhances excitability in prefrontal cortical pyramidal neurons in a state-dependent manner. Neuroscience 104:335–346. CrossRef Medline

Lebedev MA, Messinger A, Kralik JD, Wise SP (2004) Representation of attended versus remembered locations in prefrontal cortex. PLoS Biol 2:e365. CrossRef Medline

Lee I, Kesner RP (2003) Time-dependent relationship between the dorsal hippocampus and the prefrontal cortex in spatial memory. J Neurosci 23:1517–1523. Medline

Lörincz A, Notomi T, Tamás G, Shigemoto R, Nusser Z (2002) Polarized and compartment-dependent distribution of HCN1 in pyramidal cell dendrites. Nat Neurosci 5:1185–1193. CrossRef Medline

Magee JC (1998) Dendritic hyperpolarization-activated currents modify the integrative properties of hippocampal CA1 pyramidal neurons. J Neurosci 18:7613–7624. Medline

Magee JC (1999) Dendritic lh normalizes temporal summation in hippocampal CA1 neurons. Nat Neurosci 2:508–514. CrossRef Medline

Mao BQ, Hamzei-Sichani F, Aronov D, Froemke RC, Yuste R (2001) Dynamics of spontaneous activity in neocortical slices. Neuron 32:883–898. CrossRef Medline

Marder E, Calabrese RL (1996) Principles of rhythmic motor pattern generation. Physiol Rev 76:687–717. Medline

Metherate R, Cox CL, Ashe JH (1992) Cellular bases of neocortical activation: modulation of neural oscillations by the nucleus basalis and endogenous acetylcholine. J Neurosci 12:4701–4711. Medline

Miller EK, Erickson CA, Desimone R (1996) Neural mechanisms of visual working memory in prefrontal cortex of the macaque. J Neurosci 16:5154–5167. Medline

Niki H (1974) Differential activity of prefrontal units during right and left delayed response trials. Brain Res 70:346–349. CrossRef Medline

Niki H, Watanabe M (1976) Prefrontal unit activity and delayed response: relation to cue location versus direction of response. Brain Res 105:79–88. CrossRef Medline

Nolan MF, Malleret G, Lee KH, Gibbs E, Dudman JT, Santoro B, Yin D, Thompson RF, Siegelbaum SA, Kandel ER, Morozov A (2003) The hyperpolarization-activated HCN1 channel is important for motor learning and neuronal integration by cerebellar Purkinje cells. Cell 115:551–564. CrossRef Medline

Nolan MF, Malleret G, Dudman JT, Buhl DL, Santoro B, Gibbs E, Vronskaya S, Buzsáki G, Siegelbaum SA, Kandel ER, Morozov A (2004) A behavioral role for dendritic integration: HCN1 channels constrain spatial memory and plasticity at inputs to distal dendrites of CA1 pyramidal neurons. Cell 119:719–732. CrossRef Medline

Nolan MF, Dudman JT, Dodson PD, Santoro B (2007) HCN1 channels control resting and active integrative properties of stellate cells from layer II of the entorhinal cortex. J Neurosci 27:12440–12451. CrossRef Medline

Porter MC, Mair RG (1997) The effects of frontal cortical lesions on remembering depend on the procedural demands of tasks performed in the radial arm maze. Behav Brain Res 87:115–125. CrossRef Medline

Postle BR (2006) Working memory as an emergent property of the mind and brain. Neuroscience 139:23–38. CrossRef Medline

Pressler RT, Strowbridge BW (2006) Blanes cells mediate persistent feedfor-

ward inhibition onto granule cells in the olfactory bulb. Neuron 49:889–904. CrossRef Medline

Quintana J, Yajeya J, Fuster JM (1988) Prefrontal representation of stimulus attributes during delay tasks. I. Unit activity in cross-temporal integration of sensory and sensory-motor information. Brain Res 474:211–221. CrossRef Medline

Ramos BP, Birnbaum SG, Lindenmayer I, Newton SS, Duman RS, Arnsten AF (2003) Dysregulation of protein kinase a signaling in the aged prefrontal cortex: new strategy for treating age-related cognitive decline. Neuron 40:835–845. CrossRef Medline

Rigdon GC, Pirch JH (1984) Microinjection of procaine or GABA into the nucleus basalis magnocellularis affects cue-elicited unit responses in the rat frontal cortex. Exp Neurol 85:283–296. CrossRef Medline

Robinson RB, Siegelbaum SA (2003) Hyperpolarization-activated cation currents: from molecules to physiological function. Annu Rev Physiol 65:453–480. CrossRef Medline

Rowe JB, Toni I, Josephs O, Frackowiak RS, Passingham RE (2000) The prefrontal cortex: response selection or maintenance within working memory? Science 288:1656–1660. CrossRef Medline

Sakurai Y, Sugimoto S (1986) Multiple unit activity of prefrontal cortex and dorsomedial thalamus during delayed go/no-go alternation in the rat. Behav Brain Res 20:295–301. CrossRef Medline

Sánchez-Alonso JL, Halliwell JV, Colino A (2008) ZD 7288 inhibits T-type calcium current in rat hippocampal pyramidal cells. Neurosci Lett 439: 275–280. CrossRef Medline

Sanchez-Vives MV, McCormick DA (2000) Cellular and network mechanisms of rhythmic recurrent activity in neocortex. Nat Neurosci 3:1027–1034. CrossRef Medline

Santoro B, Chen S, Luthi A, Pavlidis P, Shumyatsky GP, Tibbs GR, Siegelbaum SA (2000) Molecular and functional heterogeneity of hyperpolarization-activated pacemaker channels in the mouse CNS. J Neurosci 20:5264–5275. Medline

Saxe MD, Malleret G, Vronskaya S, Mendez I, Garcia AD, Sofroniew MV, Kandel ER, Hen R (2007) Paradoxical influence of hippocampal neurogenesis on working memory. Proc Natl Acad Sci U S A 104:4642–4646. CrossRef Medline

Schwindt PC, Spain WJ, Foehring RC, Chubb MC, Crill WE (1988) Slow conductances in neurons from cat sensorimotor cortex in vitro and their role in slow excitability changes. J Neurophysiol 59:450–467. Medline

Seamans JK, Nogueira L, Lavin A (2003) Synaptic basis of persistent activity in prefrontal cortex in vivo and in organotypic cultures. Cereb Cortex 13:1242–1250. CrossRef Medline

Seamari Y, Narváez JA, Vico FJ, Lobo D, Sanchez-Vives MV (2007) Robust off- and online separation of intracellularly recorded up and down cortical states. PLoS One 2:e888. CrossRef Medline

Seeger T, Fedorova I, Zheng F, Miyakawa T, Koustova E, Gomeza J, Basile AS, Alzheimer C, Wess J (2004) M2 muscarinic acetylcholine receptor knock-out mice show deficits in behavioral flexibility, working memory, and hippocampal plasticity. J Neurosci 24:10117–10127. CrossRef Medline

Sidiropoulou K, Lu FM, Fowler MA, Xiao R, Phillips C, Ozkan ED, Zhu MX, White FJ, Cooper DC (2009) Dopamine modulates an mGluR5-mediated depolarization underlying prefrontal persistent activity. Nat Neurosci 12:190–199. CrossRef Medline

Spencer DG Jr, Pontecorvo MJ, Heise GA (1985) Central cholinergic involvement in working memory: effects of scopolamine on continuous nonmatching and discrimination performance in the rat. Behav Neurosci 99:1049–1065. CrossRef Medline

Steriade M, Amzica F, Nuñez A (1993a) Cholinergic and noradrenergic modulation of the slow (~0.3 Hz) oscillation in neocortical cells. J Neurophysiol 70:1385–1400. Medline

Steriade M, Nuñez A, Amzica F (1993b) A novel slow (< 1 Hz) oscillation of neocortical neurons *in vivo*: depolarizing and hyperpolarizing components. J Neurosci 13:3252–3265. Medline

Stuart G, Spruston N (1998) Determinants of voltage attenuation in neocortical pyramidal neuron dendrites. J Neurosci 18:3501–3510. Medline

Tahvildari B, Fransén E, Alonso AA, Hasselmo ME (2007) Switching between "On" and "off" states of persistent activity in lateral entorhinal layer III neurons. Hippocampus 17:257–263. CrossRef Medline

Valenti O, Grace AA (2009) Entorhinal cortex inhibits medial prefrontal cortex and modulates the activity states of electrophysiologically characterized pyramidal neurons in vivo. Cereb Cortex 19:658–674. CrossRef Medline

Wall PM, Messier C (2001) Methodological and conceptual issues in the use of the elevated plus-maze as a psychological measurement instrument of animal anxiety-like behavior. Neurosci Biobehav Rev 25:275–286. CrossRef Medline

Wang XJ (2001) Synaptic reverberation underlying mnemonic persistent activity. Trends Neurosci 24:455–463. CrossRef Medline

Wang M, Ramos BP, Paspalas CD, Shu Y, Simen A, Duque A, Vijayraghavan S, Brennan A, Dudley A, Nou E, Mazer JA, McCormick DA, Arnsten AF (2007) Alpha2A-adrenoceptors strengthen working memory networks by inhibiting cAMP-HCN channel signaling in prefrontal cortex. Cell 129:397–410. CrossRef Medline

Wang M, Gamo NJ, Yang Y, Jin LE, Wang XJ, Laubach M, Mazer JA, Lee D, Arnsten AF (2011) Neuronal basis of age-related working memory decline. Nature 476:210–213. CrossRef Medline

Watanabe M (1981) Prefrontal unit activity during delayed conditional discriminations in the monkey. Brain Res 225:51–65. CrossRef Medline

Watanabe M (1996) Reward expectancy in primate prefrontal neurons. Nature 382:629–632. CrossRef Medline

Williams SR, Stuart GJ (2000) Site independence of EPSP time course is mediated by dendritic I(h) in neocortical pyramidal neurons. J Neurophysiol 83:3177–3182. Medline

Winograd M, Destexhe A, Sanchez-Vives MV (2008) Hyperpolarization-activated graded persistent activity in the prefrontal cortex. Proc Natl Acad Sci U S A 105:7298–7303. CrossRef Medline

Yoshida M, Hasselmo ME (2009) Persistent firing supported by an intrinsic cellular mechanism in a component of the head direction system. J Neurosci 29:4945–4952. CrossRef Medline